UNIVERSIDADE FEDERAL DE PARAÍBA
CENTRO DE INFORMÁTICA
PROGRAMA DE PÓS-GRADUAÇÃO EM INFORMÁTICA

THULIO GUILHERME SILVA DE AMORIM

SELF-ORGANIZED FLOCKING CONTROL FOR MICRO AERIAL VEHICLES SWARM IN GLOBAL NAVIGATION SATELLITE SYSTEM-DENIED ENVIRONMENTS

JOÃO PESSOA
2021

THULIO GUILHERME SILVA DE AMORIM

SELF-ORGANIZED FLOCKING CONTROL FOR MICRO AERIAL VEHICLES SWARM IN GLOBAL NAVIGATION SATELLITE SYSTEM-DENIED ENVIRONMENTS

Dissertação submetida à Coordenação do Curso de Pós-Graduação em Informática – PPGI, da Universidade Federal da Paraíba – UFPB, como parte dos requisitos necessários para obtenção do grau de Mestre em Informática.

Orientador: Prof. Dr. Tiago P. do Nascimento

JOÃO PESSOA
2021

Catalogação na publicação
Seção de Catalogação e Classificação

A524s Amorim, Thulio Guilherme Silva de.
Self-organized flocking control for micro aerial vehicles swarm in Global Navigation Satellite System-denied environments / Thulio Guilherme Silva de Amorim. - João Pessoa, 2021.
56 f. : il.

Orientação: Tiago Pereira do Nascimento.
Dissertação (Mestrado) - UFPB/CI.

1. Swarm robotics. 2. Flocking. 3. Micro aerial vehicles. 4. Unmanned aerial vehicles. 5. Self-organization. I. Nascimento, Tiago Pereira do. II. Título.

UFPB/BC CDU 004.896(043)

Elaborado por WALQUELINE DA SILVA ARAUJO - CRB-15/514

UNIVERSIDADE FEDERAL DA PARAÍBA
CENTRO DE INFORMÁTICA
PROGRAMA DE PÓS-GRADUAÇÃO EM INFORMÁTICA

Ata da Sessão Pública de Defesa de Dissertação de Mestrado de Thulio Guilherme Silva de Amorim, candidato ao título de Mestre em Informática na Área de Sistemas de Computação, realizada em 22 de julho de 2021.

Aos vinte e dois dias do mês de julho do ano de dois mil e vinte e um, às oito horas, por meio de videoconferência, reuniram-se os membros da Banca Examinadora constituída para julgar o trabalho do sr. Thulio Guilherme Silva de Amorim, vinculado a esta Universidade sob a matrícula nº 20201003695, candidato ao grau de Mestre em Informática, na área de "Sistemas de Computação", na linha de pesquisa "Sinais, Sistemas Digitais e Gráficos", do Programa de Pós-Graduação em Informática, da Universidade Federal da Paraíba. A comissão examinadora foi composta pelos professores: Tiago Pereira do Nascimento (PPGI), orientador e presidente da banca; Alisson Vasconcelos de Brito (PPGI), Examinador Interno; Ewerton Monteiro Salvador (UFPB), Examinador Externo ao Programa; Alexandre Santos Brandão (UFV), Examinador Externo à Instituição. Dando início aos trabalhos, o Presidente da Banca cumprimentou os presentes, comunicou aos mesmos a finalidade da reunião e passou a palavra ao candidato para que o mesmo fizesse a exposição oral do trabalho de dissertação intitulado: "Uma Abordagem para Enxame Auto-Organizado de Micro Veículos Aéreos". Concluída a exposição, o candidato foi arguido pela Banca Examinadora que emitiu o seguinte parecer: "***aprovado***". Do ocorrido, eu, Ruy Alberto Pisani Altafim, Coordenador do Programa de Pós-Graduação em Informática, lavrei a presente ata que vai assinada por mim e pelos membros da banca examinadora. João Pessoa, 22 de julho de 2021.

Prof. Dr. Ruy Alberto Pisani Altafim

Prof. Tiago Pereira do Nascimento
Orientador (PPGI-UFPB)

Prof. Alisson Vasconcelos de Brito
Examinador Interno (PPGI-UFPB)

Prof. Ewerton Monteiro Salvador
Examinador Externo ao Programa (UFPB)

Prof. Alexandre Santos Brandão
Examinador Externo à Instituição (UFV)

To my parents, Luciano Amorim and Ana Patrícia Amorim, and to my stepmother, Beatriz Dulce Amorim.

Acknowledgements

To the Multi-Robot Systems (MRS) group, in particular to Pavel Petracek and Martin Saska, for the assistance in the development by instructing us how to use the MRS UAV System to set up realistic simulations and in the perform of the experiments with real robots by supplying the required equipment and personal knowledge.

To the Technology Innovation Institute (TII), particularly Eliseo Ferrante and Giulia De Masi, for help with their knowledge about swarm robotics and the revision of this work.

To my advisor, Tiago Nascimento, for the guidance during this work and for creating the connection between all those who actively contributed.

To the Coordenação de Aperfeiçoamento de Pessoas de Nível Superior (CAPES) for the financial support during the development of this work.

"Everyone fails at who they're supposed to be, Thor.
The measure of a person, a hero,
is how well they succeed at being who they are."
(FEIGE, KEVIN; ***AVENGERS: ENDGAME****, 2019)*

Resumo

Flocking, também conhecido como movimento coordenado, é um comportamento coletivo que consiste em um grande grupo de indivíduos movendo-se juntos numa direção-alvo. Os controladores de movimento coordenado para Veículos Aéreos Não-Tripulados (VANTs) contam com o Sistema Global de Navegação por Satélite (SGNS) e a comunicação intra-robô para obter as informações relativas absolutas dos robôs próximos. Esta abordagem é aplicável apenas em ambientes externos conhecidos e acessíveis. Nesta dissertação, exploramos a possibilidade de atingir movimento coordenado utilizando uma equipe de VANTs em locais de difícil acesso, particularmente em ambientes com restrições de sensoriamento remoto. Assim, propomos um método baseado em controle proximal para movimento coordenado auto-organizado de VANTs que emprega um sistema de localização relativa baseado em visão proposto por Walter, Saska and Franchi (2018) conhecido como sistema Ultra-Violet Direction And Ranging (UVDAR). Os robôs usam uma função potencial de Lennard-Jones para manter a coesão do grupo, evitando a colisão entre os companheiros. Após inúmeras simulações de ajuste e verificação de segurança, avaliamos nosso método proposto em um ambiente de mundo real com um grupo de VANTs de médio porte usando duas abordagens distintas de detecção relativa intra-enxame. Em ambos os casos, nosso método atingiu com eficiência o movimento coordenado sem controle de alinhamento e direção e se moveu em uma direção arbitrária. Desta forma, obtivemos movimento coordenado auto-organizado com informações sensoriais limitadas para robôs aéreos com alta dinâmica em ambientes sem restrições nas condições de fronteira. Como contribuições, temos uma extensão do trabalho do Ferrante *et al.* (2012) e um método de controle de movimento coordenado descentralizado com sensoriamento local capaz de funcionar em ambientes com restrição de SGNS.

Palavras-chave: Robótica de enxame. Movimento coordenado. Micro veículos aéreos. Veículos aéreos não-tripulados. Auto-organização.

Abstract

Flocking, also known as coordinated motion, is a collective behavior that consists of a large group of individuals moving together towards the same target direction. Unmanned Aerial Vehicle (UAV) flocking controllers have relied on Global Navigation Satellite System (GNSS) and intra-robot communication to obtain the absolute relative information of the nearby robots. This approach is only applicable in known and accessible outdoor environments. In this thesis, we explore the possibility of achieving flocking using a team of UAVs in hard-to-access locations, particularly with remote sensing restrictions. Thus, we propose a proximal control-based method for UAV self-organized flocking that relies on a vision-based relative localization approach proposed by Walter, Saska and Franchi (2018) called the Ultra-Violet Direction And Ranging (UVDAR) system. Robots use a Lennard-Jones potential function to maintain the cohesiveness of the flocking while avoiding collision within the teammates. After numerous simulations for safe verification and tuning, we evaluate our proposed method in a real-world environment with a group of middle-size UAVs using two distinct intra-swarm relative sensing approaches. In both cases, our method efficiently achieves flocking without alignment and direction control and moves into an arbitrary direction. In this way, we accomplished self-organized flocking with limited sensory information for aerial robots with high dynamics in environments with no constraints on the boundary conditions. As contributions, we have an extension of the work of Ferrante *et al.* (2012) and a decentralized flocking control method with local sensing capable of work in environments with GNSS restriction.

Keywords: Swarm robotics. Flocking. Micro aerial vehicles. Unmanned aerial vehicles. Self-organization.

List of Figures

List of Tables

List of abbreviations and acronyms

2-D	Two-Dimensional
3-D	Three-Dimensional
APD	Area Parts Database
DOF	Degree of Freedom
GCS	Ground Control Station
GNSS	Global Navigation Satellite System
GPS	Global Positioning System
MAV	Micro Aerial Vehicle
MDMC	Magnitude-dependent Motion Control
MPC	Model Predictive Control
MRS	Multi-Robot Systems
ROS	Robot Operating System
SLERP	Spherical Linear Interpolation
UAV	Unmanned Aerial Vehicle
UGV	Unmanned Ground Vehicle
UV	Ultra-Violet
UVDAR	Ultra-Violet Direction And Ranging

List of symbols

a_d	Unbiased desired acceleration (m/s^2)
α	Steepness of the Lennard-Jones potential function P_i
$\mathbf{b}$	Vectorial sum of the headings of a group of robots
B_s	Forward biasing speed (m/s)
χ_d	Desired control reference
d	Relative range of a perceived robot or obstacle (m)
δ	Accuracy metric
d_{des}	Desired inter-robot distance (m)
D_e	Effective traveled distance metric (m)
D_p	Maximum interaction distance (m)
e	Number of Euler
ϵ	Strength of the Lennard-Jones potential function P_i
η_d	Desired heading angle of the UAV in the world frame (rad)
η_p	Physical heading angle of the UAV in the world frame (rad)
η_s	Smoothed heading angle of the UAV in the world frame (rad)
f_x	Projection of the proximal control vector $\mathcal{P}$ on the X-plane of the body reference frame of the focal robot
f_y	Projection of the proximal control vector $\mathcal{P}$ on the Y-plane of the body reference frame of the focal robot
g	Gravitational acceleration (m/s^2)
γ	SLERP interpolation coefficient
$\mathbf{h}$	Heading vector of the UAV
j	Imaginary unit
k	Number of robots and obstacles perceived by the robot's sensors

K_1	MDMC linear gain (m/s)
K_2	MDMC angular gain (rad/s)
λ	Positive gain that limits the maximum interaction distance D_p
m	Nominal UAV mass (kg)
m_p	Number of neighboring robots perceived within the maximum interaction distance D_p
$\bar{\mu}$	Steady-state metric
N	Number of robots in the flock
ω	Angular velocity of a UAV in the body frame (rad/s)
ω_d	Desired intrinsic angular velocities of the UAV (rad/s)
Ω	Tensor of angular velocity
p_i	Negative derivate of the generalized version of the Lennard-Jones potential function P_i
P_i	Generalized version of the Lennard-Jones potential function
$\mathcal{P}$	Proximal control vector
ϕ	Relative bearing of a perceived robot or obstacle (rad)
ψ	Order metric
q_p	Quaternion of the physical heading angle of the UAV in the world frame
q_s	Quaternion of the smoothed heading angle of the UAV in the world frame
$\mathbf{r}$	Position of the center of mass of a UAV in the world frame (m)
$\dot{\mathbf{r}}$	Velocity of the center of mass of a UAV in the world frame
$\ddot{\mathbf{r}}$	Acceleration of the center of mass of a UAV in the world frame
$\mathbf{r}_d$	Desired position of the center of mass of a UAV in the world frame (m)
R	Estimated orientation of the UAV with heading
σ	Amount of noise of the Lennard-Jones potential function P_i
t	Time (s)

t^*	Settling time metric (s)
T	Duration of the experiments (s)
$\mathbf{T}_d$	Desired collective motor speed
τ_d	Desired individual motor speed of all motors
θ	Angle between the quaternion of the smoothed heading angle q_s and the quaternion of the physical heading angle q_p (rad)
u	Desired linear translational speed of the UAV from the flocking controller (m/s)
v	Desired angular speed of the UAV from the flocking controller (rad/s)
v_i	Negative derivative of a virtual potential function
$\mathcal{V}$	Virtual force vector
x	Estimated state vector
z_{coeff}	Desired height in the body frame of the UAV (m)

Contents

1 Introduction

Coordinated motion, also known as flocking, is a collective behavior that consists of a large group of individuals moving together towards the same target direction. It can be observed in different species in nature, and replicate this behavior using robots has been an active research topic inspired by how easily simple individuals with limited resources can achieve complex organizations.

The combination of this basic behavior with others can tackle a variety of complex real-world applications. For a group of autonomous robots, coordinated motion can be an effective way to navigate in an environment with limited or no collisions between robots (BRAMBILLA *et al.*, 2013). When designed as a swarm robotics system, the flocking, as a global behavior, emerges from local interactions between the robots and the environment in a distributed manner. The robots rely only on onboard sensors and make their decisions locally, without centralized control, using a set of simple rules.

1.1 Motivation

Developing flocking control for Unmanned Ground Vehicles (UGVs) has achieved the highest stage of maturity. The works of Turgut *et al.* (2008) and Ferrante *et al.* (2012) presented effective methods for accomplishing ordered and cohesive flocking using a combination of decentralized control and local sensing. However, design controls with similar attributes for Unmanned Aerial Vehicles (UAVs) are still an open challenge.

A fundamental component in robot behavior necessary to implement flocking is the ability to measure the distance and relative orientation of neighboring robots (BAYINDIR, 2016). Due to simplicity, previous works using UAVs have relied on remote position sensing, such as Global Navigation Satellite Systems (GNSSs), and intra-robot communication to obtain the absolute relative information of the nearby robots in outdoor environments.

These solutions provide precise mutual position information with the drawback of requiring preinstalled infrastructures, limiting the usage to known, uncluttered, and easily accessible environments. Additionally, they are costly and tend to rely on intensive radio communication, which is subject to limited range and interferences (WALTER; SASKA; FRANCHI, 2018). Several tasks, especially when it involves exploration, cannot rely on these solutions (COPPOLA *et al.*, 2020).

In this work, we explore the possibility of achieving flocking using a team of UAVs in hard-to-access locations, particularly in environments with remote sensing restrictions. The capability to deal with this kind of environment increases the application range of the

flocking as a navigation behavior.

1.2 Objectives

1.2.1 Main Objective

The main objective of this work is to develop a decentralized flocking control system that enables cohesive and ordered navigation with multiple UAVs and does not rely on remote sensing.

1.2.2 Secondary Objectives

The secondary objectives to reach the main one are:

- Develop a decentralized control system that enables coordinated motion with multiples flying robots. For that, we extend the work of Ferrante *et al.* (2012) by adapting their method for UAVs;
- Employ a relative localization system that does not depend on remote sensing. We aim to use a vision-based relative localization approach proposed by Walter, Saska and Franchi (2018) called the Ultra-Violet Direction And Ranging (UVDAR) system to accomplish local relative sensing.

1.3 Dissertation Structure

The rest of this dissertation is arranged as follows. In Chapter 2, we give a brief introduction of the related subjects to assist the understanding of our method. We present an overview of multirotor UAVs, which is the type of robot used. Additionally, we outline the topic of swarm robotics, a field of research that aims to develop robotics systems that exhibit natural behaviors. We also describe flocking behavior as a whole. In Chapter 3, we review the related researches. We start with flocking methods designed for UGVs since early contributions were achieved using this kind of robot. Then, we explain the flocking methods developed for UAVs. In Chapter 4, we detail the proposed decentralized flocking control and how we assembled it with the UAV overall system. In Chapter 5, we describe the implementation, the metrics, the simulation and the real robot experimental setup, and the results. Then, we also discuss the whole work. Finally, we conclude our work in Chapter 6.

2 Theoretical Concepts and Foundations

In this chapter, we present the theoretical concepts and foundations. In Section 2.1, we introduce the concepts of UAVs. In Section 2.2, we explain the topic of swarm robotics and its relation with flocking. In Section 2.3, we describe flocking as a collective behavior and how it is accomplished with robots as individuals.

2.1 Multirotor Unmanned Aerial Vehicles

Aerial robotics is a fast-growing field of robotics. Multirotor aircraft, such as the quad-rotor, is rapidly growing in popularity. Quad-rotor aerial robotic vehicles have become a standard platform for robotics research worldwide. They already have sufficient payload and flight endurance to support several indoor and outdoor applications. The improvements of batteries and other technology are rapidly increasing the scope for commercial opportunities. They are highly maneuverable and enable safe and low-cost experimentation in mapping, navigation, and control strategies for robots that move in Three-Dimensional (3-D) space. This ability to move in a 3-D space brings new research challenges compared with the wheeled mobile robots, which have driven mobile robotics research over the last decade. Small quad-rotors have been demonstrated for exploring and mapping 3-D environments, transporting, manipulating, and assembling objects, and acrobatic tricks such as juggling, balancing and flips. Additional rotors can be added to improve payload and reliability, leading to generalized N-rotor vehicles (MAHONY; KUMAR; CORKE, 2012).

Unmanned multirotor aircraft systems have been studied extensively in recent years (LEE; KIM, 2017; SHRAIM; AWADA; YOUNESS, 2018). One of the main reasons for this is their high mobility and their capacity to perform tasks with complete autonomy. Furthermore, due to several limitations characterizing these vehicles, such as their under-actuation, low computational power, high working frequency, low autonomy, and so on, they make ideal test-beds for innovative theoretical approaches to the problem of controlling mechanical systems (L'AFFLITTO; ANDERSON; MOHAMMADI, 2018).

2.2 Swarm Robotics

Swarm robotics is the study of how a large number of relatively simple physically embodied agents can be designed such that a desired collective behavior emerges from the

Figure 1 – A schematic representation of a quad-rotor with A as the reference point, $\mathbb{I}$ as the inertial reference frame and $\mathbb{J}$ is the robot's reference frame

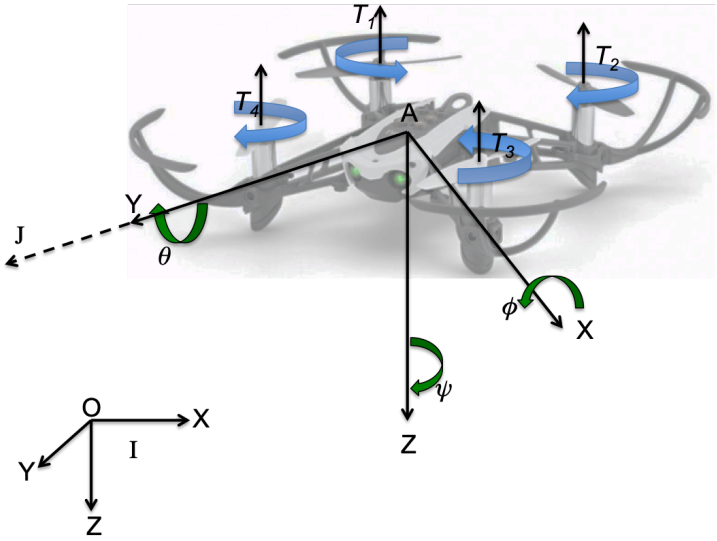

Source: Elaborated by the Author

local interactions among the agents and between the agents and the environment (ŞAHIN, 2005). It takes inspiration from the collective behavior observed in nature in many living species, where local interaction between individuals and with the environment leads a group of autonomous agents to solve complex tasks in a distributed manner, without a central control unit (BAYINDIR, 2016).

Analogous to groups of social animals, a swarm of robots should feature three functional attributes:

- Robustness: the swarm robotic system should continue to operate, although at lower performance, despite failures in the individuals, or disturbances in the environment (ŞAHIN, 2005);
- Scalability: the swarm should operate under a wide range of group sizes (ŞAHIN, 2005), and the introduction or removal of individuals does not result in a drastic change in performance (BRAMBILLA *et al.*, 2013);
- Flexibility: the swarm should cope with a broad spectrum of different environments and tasks (BRAMBILLA *et al.*, 2013).

Together with other collective behaviors in swarm robotics, flocking have as typical applications: UAV controlling, post-disaster relief, geological survey, and military applications (TAN; ZHENG, 2013). Concerning Micro Aerial Vehicles (MAVs), these global behaviors include, but are not limited to: collaborative transport and object manipulation,

collaborative construction, distributed sensing, and parallelized exploration and mapping of environments (COPPOLA *et al.*, 2020).

2.3 Flocking

Coordinated motion, also known as flocking, can be defined as the cohesive and ordered movement of a group of individuals in a common direction (REYNOLDS, 1987). It is one of the collective behaviors studied in the field of swarm robotics and focuses on how to organize and coordinate the movement of a swarm of robots (BRAMBILLA *et al.*, 2013).

Flocking can be observed in nature in many bird species, fish schooling, and the formation of herds in ungulates (BAYINDIR, 2016). More precise navigation, reduced energy consumption, and increase survival rate are some of the advantages for animals obtained through flocking (BRAMBILLA *et al.*, 2013).

There are still no formal or precise ways to design the local interactions that produce any collective behavior. However, flocking generally draws inspiration from artificial physics (BRAMBILLA *et al.*, 2013). Artificial physics is a field of research that models the behavior of individual agents using virtual forces. These forces determine the movement of agents, and consequently, the interactions between agents and the surrounding environment (BAYINDIR, 2016). Although the forces are virtual, agents act as if they were real. Thus the agent's sensors must see enough to allow it to compute the force to which it is reacting. The agent's effectors must allow it to respond to this perceived force (SPEARS *et al.*, 2004). Each robot perceives neighboring robots and obstacles and estimates their distance and relative position. Then, the robot computes a virtual force vector $\mathcal{V}$ as described in Equation 2.1 (BRAMBILLA *et al.*, 2013).

$$\mathcal{V} = \sum_{i=1}^{k} v_i(d_i)e^{j\phi_i} \tag{2.1}$$

Where: $v_i(d_i)e^{j\phi_i}$ is a vector expressed in the complex plane, ϕ_i and d_i are, respectively, the relative bearing and range of the ith perceived robot or obstacle, k is the number of robots and obstacles perceived, and $v_i(d_i)$ is the negative derivative of a virtual potential function.

A virtual potential function, also known as artificial potential function, is often used in swarm robotics and statistical physics to model social interaction between robots or between particles (FERRANTE *et al.*, 2012). The most commonly used virtual potential is the Lennard-Jones potential (BRAMBILLA *et al.*, 2013). The Lennard-Jones potential function models two distinct forces between neutral molecules and atoms, and either neutral molecules or atoms. The forces are based on the distances between the molecules:

the attractive force makes the molecules move closer at long ranges, and the repulsive force makes the molecules move apart at short ranges, causing the molecules to maintain a natural balance (SPEARS *et al.*, 2004). A generalized version of the Lennard-Jones potential function $P_i(d_i)$ is computed as (FERRANTE *et al.*, 2012):

$$P_i(d_i) = 4\epsilon \left[\left(\frac{\sigma}{d_i} \right)^{2\alpha} - \left(\frac{\sigma}{d_i} \right)^{\alpha} \right] \tag{2.2}$$

Where: ϵ is the strength of the potential function, α is the steepness of the potential function, and σ is the amount of noise.

The Lennard-Jones function behavior as follows: when $d_i = 2^{\frac{1}{\alpha}}\sigma$, the interaction energy between two robots is at zero. When $d_i > 2^{\frac{1}{\alpha}}\sigma$, the interaction energy decreases to -1 and then increases and eventually reaches zero at longer range, causing non-interaction. When $d_i < 2^{\frac{1}{\alpha}}\sigma$, the interaction energy is very high, reaching infinite (SPEARS *et al.*, 2004). We calculate the negative derivative of the generalized version of the Lennard-Jones potential function $p_i(d_i)$ as (FERRANTE *et al.*, 2012):

$$p_i(d_i) = -\frac{\partial P(d_i)}{\partial d_i} = -\frac{4\alpha\epsilon}{d_i} \left[2\left(\frac{\sigma}{d_i} \right)^{2\alpha} - \left(\frac{\sigma}{d_i} \right)^{\alpha} \right] \tag{2.3}$$

Since the force interaction between two robots is zero when $d_i = 2^{\frac{1}{\alpha}}\sigma$, to impose the robots to maintain a desire inter-robot distance using the Lennard-Jones force function, we calculate the amount of noise σ as:

$$\sigma = \frac{d_{des}}{2^{\frac{1}{\alpha}}} \tag{2.4}$$

Where: d_{des} is the desired inter-robot distance.

When using the negative derivate of the Lennard-Jones potential function, each robot interacts with its surrounding in three distinct manners. It moves to the opposite direction of the force when $d_i < 2^{\frac{1}{\alpha}}\sigma$. Alternatively, it goes in the direction of the force when $d_i > 2^{\frac{1}{\alpha}}\sigma$. When $d_i = 2^{\frac{1}{\alpha}}\sigma$, the force does not affect the robot.

3 Related Researches

Reynolds (1987) published one of the early works about flocking in the domain of computer graphics. In his paper, three basic rules are carried out by each individual in the swarm to accomplish the flocking: separation rule, cohesion rule, and alignment rule. The separation rule forces the individual to maintain a distance from its neighbors to avoid collisions. The cohesion rule allows the individual to stay close to its neighbors to keep the group together. The alignment rule aligns the individual's heading with the average heading of its neighbors.

The most common use of the Reynolds' rules in flocking is in the form of virtual forces (TAN; ZHENG, 2013). As one of the first works, Khatib (1986) used the concept of an artificial potential field. In his work, a PUMA 560 robot manipulator moves in a field of forces. The position to be reached performs an attraction force while the obstacles perform a repulsion force.

Spears *et al.* (2004) introduced a virtual physics-based method called *physicomimetics*, a framework for distributed control of a large number of mobile robots based on artificial physics. In one of the experiments with real robots, a group of seven robots moves toward a light source while keeping a self-organized hexagon formation. Each robot uses an infrared sensor to estimate the relative bearing and distance of each neighboring robot. Then, the robot computes the attraction or repulsion force using the Newtonian force law. As the final step, the robot responded by turning or moving to some position.

Turgut *et al.* (2008) developed a self-organized flocking for a swarm of robots using proximal and heading control. The robot uses an infrared sensor to measure the relative distance and bearing of the nearby robots and distinguish robots from obstacles. Later, the proximal control, which encodes the separation and cohesion rules, uses this information to maintain a desired distance from the nearby robots and avoid obstacles. The robot also utilizes a sensor called Virtual Heading Sensor. The Virtual Heading Sensor uses a digital compass to estimate the robot heading in a clockwise direction concerning the sensed North and broadcast it to the neighboring robots inside the communication range. The heading control, which encodes the alignment rule, aligns the robot heading with the average of its neighbors. The combination of the proximal and heading control generates the desired heading vector. Then, the motion control translates the desired heading vector into a forward and angular velocity.

The work of Turgut *et al.* (2008) not only was the first implementation of all Reynolds' rules (REYNOLDS, 1987) for real robots but also was the first work capable of accomplishing the flocking using only onboard sensing. The experiments used a small

group of seven physical mobile ground robots and, in the simulations, a swarm of 1000 robots.

Hettiarachchi and Spears (2009) extended the framework *physicomimetics* proposed by Spears *et al.* (2004) introducing the Lennard-Jones force law. In the results, the application of the Lennard-Jones force law as a potential function demonstrated superior performance compared with the Newtonian force law. Later, the Lennard-Jones potential function became the most commonly used function.

Çelikkanat and Şahin (2010) continued the work of Turgut *et al.* (2008) introducing the possibility of control the flocking direction using informed robots. Informed robots are a small fixed number of individuals in the swarm with knowledge of a goal direction. All robots still move forward and maintain a desired distance from the others. In addition, the informed robots have the desired direction to move.

Ferrante *et al.* (2012) proposed a self-organized flocking behavior using only the proximal control, without the alignment control, and without informed robots. The implementation of the proximal control is similar to the described by Turgut *et al.* (2008), and the contribution lies in the motion control method called Magnitude-dependent Motion Control (MDMC). In previous works, the robot moves forward with a fixed velocity and rotates based on the direction of the virtual force. However, the motion control presented by Ferrante *et al.* (2012) makes the robot move forward but also allows it to go backward depending on the direction of the virtual force. The MDMC, together with the proximal control, achieved flocking without alignment, without goal direction, and without external computation.

All those works were applied for UGVs in indoor environments (SPEARS *et al.*, 2004; TURGUT *et al.*, 2008; ÇELIKKANAT; ŞAHIN, 2010; FERRANTE *et al.*, 2012). The use of mobile ground robots in an indoor environment for testing flocking algorithms is mainly due to the simpleness of the environment setup. Still, the adaptation of the proposed methods from ground robots to flying robots is usually mentioned as future work by many authors.

Among the works involving UAV flocking algorithms, Virágh *et al.* (2014) presented a decentralized control flocking algorithm developed using a realistic simulation framework. A self-propelled flocking control generates the desired velocity vector using a short-range repulsion term to avoid collisions and a velocity alignment term to align the heading direction of nearby units. The author describes the alignment term as a viscous friction-like force that prevents instabilities, such as sensor inaccuracy or delay. The outdoor experiment was performed using nine quad-copters with an onboard computer, GPS device, and XBee module communication. Each robot extracts the required relative coordinates from the global position and velocity broadcasted using a local wireless communication without establishing one-to-one connections or a mesh network.

Kownacki and Ołdziej (2016) demonstrated a decentralized control algorithm for self-organized flocking using fixed-wing UAVs. Without the alignment rule, the cohesion and separation rules proposed by Reynolds (REYNOLDS, 1987) were combined with a leadership feature. The leadership plays a guidance role in the flocking. The leader can be a single member or a small group of individuals with information of direction, similar to the informed robots concepts, but does not follow the repulsion and cohesion rules and is fully controllable by the Ground Control Station (GCS). As individuals, the work uses two Multiplex twin-engine TwinStar with an 868 MHz radio modem XBee Pro to enable navigation data exchange between the individuals through a local wireless network, a 2.4 GHz radio modem to establish the communication between leaders and the GCS, and a GPS. Outdoor experiments were performed to evaluate the proposed method.

The work of Benedetti *et al.* (2017) developed a decentralized control for self-organized UAV flocking and area coverage mission planning. The overall mission consisted of acquiring relevant data from a specific location using the onboard sensors of the UAVs and then transmitting it to a GCS. The flocking behavior follows the Reynolds' rules (REYNOLDS, 1987): separation, cohesion, and alignment rules. The flock is highly configurable by tuning a set of parameters, which made their method suitable for distinct types of monitoring missions. Each UAV exchanges relative information among them using a gossiping and update mechanism. The gossiping mechanism consists of broadcast the local agent database, which stores the relative position of the own UAV and its nearby neighbors, to the robots through a low-power communication range. The update mechanism is responsible for updating the local database with the information received. To ensure the area coverage, each UAV also has an Area Parts Database (APD), which saves the covered area parts, and periodically sends this information to a leader robot that merges all APDs and plans the path to follow. The proposed method has been evaluated only in simulations using quad-rotors with 450 mm of inter-distance between the motors, 8 x 4.5 propellers, and a weight of 1 kg.

Vásárhelyi *et al.* (2018) proposed a decentralized UAV flocking control for confined environments. The proposed method generates a desired velocity using repulsion and velocity alignment rules. However, to maintain the individuals together, a repulsive force retains the individuals inside a bounded flight arena. In addition, a similar repulsive force describes the obstacles as a collision avoidance mechanism. The authors applied an evolutionary optimization to identify the parameters that maximize the flock's speed and coherence while minimizing the collisions. Thirty identical quad-copters equipped with a Pixwawk autopilot, an onboard minicomputer Odroid C1+, an XBee module, and GNSS receivers were applied in real-world experiments in an outdoor environment. The robots used two complementary, independent, and parallel wireless modules to inter-robot communication. The XBee module broadcasts packets with a small bandwidth but with a larger range. A Wi-Fi module embedded in the onboard PC transmits packets through a

local ad hoc wireless network with a large bandwidth but shorter range. The shared data contain the geodetic position and velocity measured by the onboard GNSS receivers, and the relative information comes from the differences of GNSS-based absolute measurements.

Silic and Mohseni (2019) introduced an atmospheric platform system for plume monitoring using fixed-wing UAVs. Since the arrangement of the sensors in the environment is crucial to obtain rich information, the main objective was to organize the UAVs equipped with onboard sensors in a cohesive formation inside the plume boundary. To explore an unknown environment, the UAVs randomly moves to a fixed position and gathering data for a while. The GCS receives from the UAVs the environmental data through wireless communication and then processes it to estimate the plume location. Also, the GCS organizes the formation by receiving their GPS coordinates and sending new positions to investigate. Once the position of the plume is well-known, they keep loitering in circles inside the plume boundary. The system was evaluated with three delta wing UAVs with a GPS receiver, a radio transceiver, a barometer, an atmospheric sensor, and a 9-axis inertial measurement unit. The UAV communicates only with the GCS using XBee radios.

In Table 1, we compare the mentioned UAV flocking algorithms and our proposed work. Flocking is often accomplished with decentralized planning using GNSS information. The work of Virágh *et al.* (2014), Kownacki and Ołdziej (2016) and Vásárhelyi *et al.* (2018) were tested through realistic simulations and real-world experiments while the work of Benedetti *et al.* (2017) was tested only using realistic simulations. With experiments using thirty physical UAVs, the work of Vásárhelyi *et al.* (2018) can be considered one of the most impressive achievements so far. However, achieving coordinated swarm behaviors without external sensing and computation is a challenging task, as has been very well explained in the recent survey of Coppola *et al.* (2020).

Table 1 – Comparison between the mentioned UAV flocking algorithms and our work

Work	**Decentralized planning**	**Real-world experiment**	**Local sensing**
Virágh *et al.* (2014)	✓	✓	
Kownacki and Ołdziej (2016)	✓	✓	
Benedetti *et al.* (2017)	✓		
Vásárhelyi *et al.* (2018)	✓	✓	
Silic and Mohseni (2019)		✓	
Our work	✓	✓	✓

Source: Elaborated by the Author

UAV swarm control is a relatively new field of research, and its applications are yet to be explored (SASKA, 2020). One of the many possibilities is the use of UAVs for inspecting hard-to-access locations, especially in GNSS-denied environments. This type of application requires the swarm coordination to be flexible and to move adaptively (see

Figure 2 – Swarms of multirotor UAV testing novel flocking algorithms

(a) Localized by a GNSS system

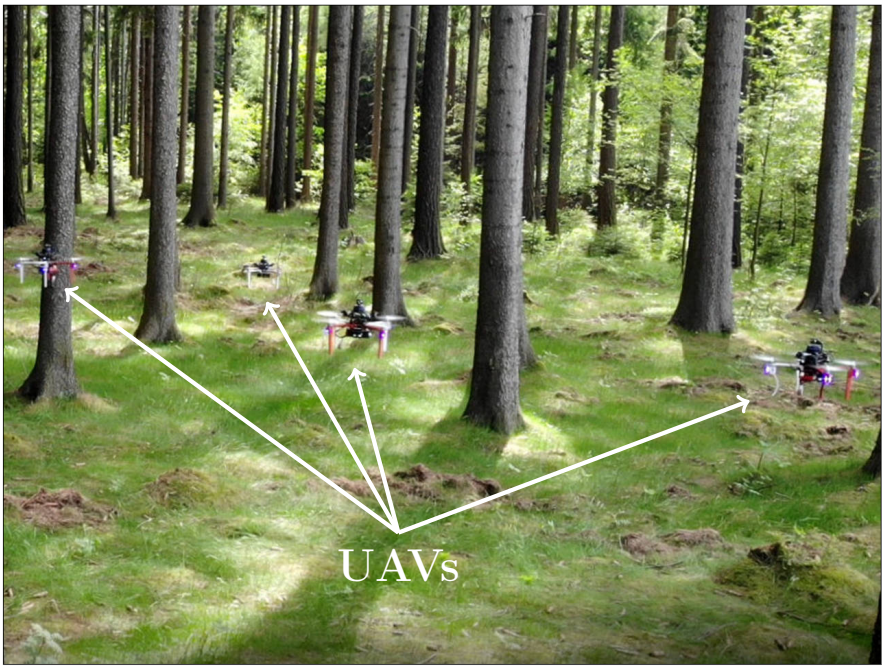

(b) Localized by onboard sensors only within a forest environment

Source: Baca *et al.* (2020)

Figure 2). This type of situation often requires a deeper study of the flocking capabilities of the UAV group.

4 Self-organized Flocking

Flocking control methods are generally composed of three different term-functions: a proximal term, an alignment term, and an optional goal direction term, which is needed when the swarm is required to steer towards a specific target. Let us assume that in a flocking of N robots, a robot i, with $i \in \{1, \ldots, N\}$, is called the focal robot. In our work, we propose a flocking control function that uses only the proximal term in order to converge and move the UAVs into a unified direction.

4.1 Proximal Control

The proximal control is used to make the UAV maintain the desired distance from other neighbor robots while keeping a cohesive formation and assumes that the focal robot can sense the relative range and bearing of its neighboring UAVs within a maximum interaction distance of D_p. For the model of Ferrante *et al.* (2012) to be properly implemented on a flocking of UAVs, we must be less or equal to the maximum sensing range of the sensor. When the swarm converges into a stable formation, interactions between UAVs are limited to the first neighbors in the Voronoi sense, which in turn mandates that $D_p = \lambda d_{des}$, where d_{des} is the desired distance between UAVs, and λ is a positive gain that limits the maximum interaction distance is less than the twice the desired distance between two robots. The proximal control computes a proximal control vector $\mathcal{P}$ as:

$$\mathcal{P} = \sum_{i=1}^{m_p} p_i(d_i) e^{j\phi_i} \tag{4.1}$$

Where: $p_i(d_i)e^{j\phi_i}$ is a vector expressed in the complex plane, $\mathcal{P}$ is a virtual force vector, $p_i(d_i)$ is the negative derivative of the generalized version of the Lennard-Jones potential function, m_p is the number of neighboring UAVs perceived by the focal robot within the maximum interaction distance D_p, and ϕ_i and d_i are, respectively, the relative bearing and range of the ith perceived robot.

4.2 Magnitude-dependent Motion Control

To pass the information calculated in the proximal control to the UAV control system, we need first to translate it into robot motion. In the following, we assume that the UAV has a translation axis x and a rotational axis y. First, we decompose the value of the proximal control vector $\mathcal{P}$ into f_x and f_y by using the values of the relative bearing ϕ.

We call f_x and f_y the projection of the proximal control vector $\mathcal{P}$ on the XY-plane of the body frame of the focal robot:

$$\begin{aligned} f_x &= \sum_{i=1}^{m_p} p_i(d_i) \cos \phi_i \\ f_y &= \sum_{i=1}^{m_p} p_i(d_i) \sin \phi_i \end{aligned} \tag{4.2}$$

After that, we employ the MDMC. The basic idea of the MDMC algorithm is to convert the flocking control vector into a desired linear translational speed u and a desired angular speed v of the robot. However, it is important to assume that the robot has a non-holonomic behavior (FERRANTE *et al.*, 2012). The desired linear translational speed u is assumed to be directly proportional to the x component of the vector (f_x), which results in the forward velocity of the robot in the body frame. Conversely, the desired angular speed v will be directly proportional to the y component of the vector (f_y). Thus, we can calculate both as:

$$\begin{aligned} u &= \kappa_1 f_x + B_s \\ v &= \kappa_2 f_y \end{aligned} \tag{4.3}$$

Where: B_s is a forward biasing speed, and κ_1 and κ_2 are the linear and angular gains, respectively.

Note here that the larger the value of f_x, the faster the robot moves forward, while the larger the value of f_y, the faster the robot turns. However, this approach also allowed the robot to move backward, although tending to move forward due to the forward biasing speed B_s.

4.3 UAV Model application

The above-mentioned sections presented how we used the approach proposed by Ferrante *et al.* (2012). The initial method was designed for non-holonomic ground robots running at a maximum speed of 0.005 m/s and a maximum distance of 0.81 m. In contrast, we propose the use of this method in a flocking of UAVs with a maximum linear velocity of 0.3 m/s and the desired distance of 6 m.

To illustrate the model of the robot, let us use a dynamical model of a multirotor aerial vehicle presented in the work of Lee, Leok and McClamroch (2010). We need this model to understand the influence of this algorithm on the behavior of the UAV. Figure 3 illustrates the coordinate frames used in this work. In this section, all variables are

Figure 3 – The image depicts the world frame $\mathcal{W} = \{\hat{\mathbf{e}}_1, \hat{\mathbf{e}}_2, \hat{\mathbf{e}}_3\}$ in which the 3-D position and the orientation of the UAV body is expressed

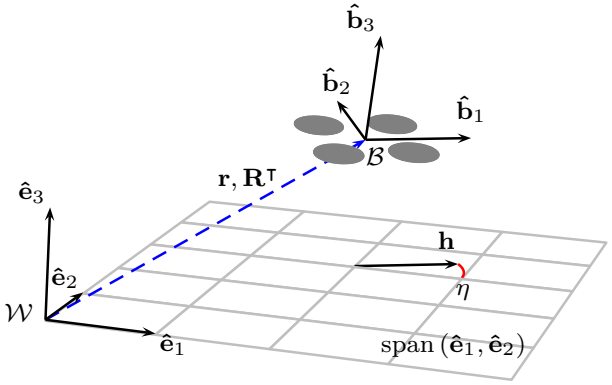

Source: Baca *et al.* (2020)

expressed in the world coordinate frame except the angular velocities ω. Our UAV feedback system architecture relies on state variables defined as:

$\mathbf{r} = [x, y, z]^\intercal$	the position of the center of the mass of a UAV in the world frame;
$\dot{\mathbf{r}} \in \mathbb{R}^3$	the velocity of the center of the mass of a UAV in the world frame;
$\ddot{\mathbf{r}} \in \mathbb{R}^3$	the acceleration of the center of a mass of a UAV in the world frame;
$\mathbf{R} \in \mathrm{SO}(3) \subset \mathbb{R}^{3\times3}$	the rotation matrix from the body frame of a UAV to the world frame, $\det \mathbf{R} = 1$, $\mathbf{R}^\intercal = \mathbf{R}^{-1}$;
$\omega = [\omega_1, \omega_2, \omega_3]^\intercal$	the angular velocity in the body frame of a UAV.

These states are linked by a nonlinear model, which has a translation part:

$$m\ddot{\mathbf{r}} = f_T \mathbf{R}\hat{\mathbf{e}}_3 + mg\hat{\mathbf{e}}_3 \tag{4.4}$$

And a rotational part:

$$\dot{\mathbf{R}} = \mathbf{R}\boldsymbol{\Omega} \tag{4.5}$$

Where: $\boldsymbol{\Omega}$ is the tensor of angular velocity, under the condition $\boldsymbol{\Omega}\,\mathbf{v} = \omega \times \mathbf{v}, \forall \mathbf{v} \in \mathbb{R}^3$. The vehicle experiences downwards gravitational acceleration with magnitude $g \in \mathbb{R}$ together with the thrust force f_T created collectively by the propellers in the direction of $\hat{\mathbf{b}}_3$.

However, as we are focused on non-aerobatic flight, we separately consider and estimate the azimuth of the $\hat{\mathbf{b}}_1$ axis in the world as the UAV *heading*. Under the condition of $|\hat{\mathbf{e}}_3^\intercal \hat{\mathbf{b}}_1| > 0$, we define the heading as:

$$\eta = \mathrm{atan2}\left(\hat{\mathbf{b}}_1^\intercal \hat{\mathbf{e}}_2, \hat{\mathbf{b}}_1^\intercal \hat{\mathbf{e}}_1\right) \tag{4.6}$$

The heading is a more intuitive alternative to the widely-used *yaw* angle as one of the 4 controllable Degrees Of Freedom (DOFs). It is possible to use the yaw, but with the assumption that the tilt of the UAV ($\cos^{-1}\ \hat{\mathbf{b}}_3^\intercal\hat{\mathbf{e}}_3$) is low, near horizontal. We do not use *Euler angles* due to the overwhelming number of conventions, which often lead to misunderstanding. Generally, the widely-used *yaw* angle (as in *Euler angles* (DIEBEL, 2006)) has no direct meaning concerning the particular orientation of any of the body axes in any of the conventions, since the final orientation also depends on the remaining two rotations (pitch, roll). A user would need to take the remaining part of the desired orientation (produced by the controllers) into account to properly design the desired *yaw*, which leads to a *chicken or egg* problem. Thus, we define the heading vector by the $\hat{\mathbf{b}}_1$ axis as:

$$\mathbf{h} = \left[\mathbf{R}_{(1,1)}, \mathbf{R}_{(2,1)}, 0\right]^\intercal = [\mathbf{b}_1^\intercal\hat{\mathbf{e}}_1, \mathbf{b}_1^\intercal\hat{\mathbf{e}}_2, 0]^\intercal \tag{4.7}$$

And its normalized form:

$$\hat{\mathbf{h}} = \frac{\mathbf{h}}{\|\mathbf{h}\|} = [\cos\eta, \sin\eta, 0]^\intercal \tag{4.8}$$

Figure 3 also illustrates the heading vector and the heading for the UAV body frame. Therefore, we can note that all these factors directly influence the calculations of range and bearing between neighboring robots, being the bearing calculation the most problematic in UAVs. Furthermore, for the algorithm to work, the robots must behave in a non-holonomic manner. Finally, the dynamic effects caused by friction between the wheels of the mobile ground robots and the floor present a major feature for the algorithm of Ferrante *et al.* (2012) to work stably, preventing the ground robots to rotate on their axis when the bearing calculates varies rapidly.

When implementing this algorithm into multirotor UAVs, one must first decrease the robot dynamics to mimic the friction effect. UAVs are highly unstable and tend to drift due to errors in state estimation. Thus, we use a system architecture that includes a Model Predictive Control (MPC) Tracker (BACA *et al.*, 2018) and a Position/Attitude controller (BACA *et al.*, 2020). We will discuss this architecture later.

However, even when stabilizing the UAV (and therefore mimicking the friction effect), the presence of a rapid variation on the bearing still presents a major problem. We re-calculate the observed heading with a Spherical Linear Interpolation (SLERP) technique to minimize this problem. SLERP represents a popular technique to interpolate between two 3-D rotations in a mathematically sounded manner while producing visually smooth

paths. Thus, the recalculation of the bearing transforms the robot physical heading angle:

$$q_s(t) = \left[\frac{\sin((1-\gamma)\theta)}{\sin\theta}\right] q_p(t) + \left[\frac{\sin(\gamma\theta)}{\sin\theta}\right] q_s(t-1) \tag{4.9}$$

Where: q_s is the quaternion of the smoothed heading angle at the instant t, q_p is the quaternion of the physical heading angle, θ is the angle between both quaternions, and γ is an interpolation coefficient.

For $\theta \approx 0$, the SLERP equation results in:

$$q_s(t) = (1-\gamma)q_p(t) + \gamma q_s(t-1) \tag{4.10}$$

Thus, we find the smoothed heading angle η_s through the quaternion of the smoothed heading angle q_s. With the problems solved, there is still the need to input the non-holonomic behavior on the UAVs. The system architecture, which will be discussed later, takes as input values the desired position and heading in the global frame. To input a non-holonomic behavior, we must input the update of the robot's position as we would in a non-holonomic robot. Therefore, we can use the smoothed heading angle η_s to update the reference position according to the equations below.

$$\begin{aligned} x_d(t) &= x + u\cos\eta_s \\ y_d(t) &= y + u\sin\eta_s \\ z_d(t) &= z_{coeff} \\ \eta_d(t) &= \eta_s + v \end{aligned} \tag{4.11}$$

Where: $[x_d, y_d, z_d]^\intercal = \mathbf{r}_d$ is the desired 3-D position of the center of the mass of the focal UAV, and η_d is the desired heading of the focal UAV, both at the instant t and in the world frame.

After calculate the desired reference $\mathbf{r}_d$ and desired heading η_d, our proposed method send it to the next block in the system architecture. Note that, similar to the work of Ferrante *et al.* (2012), the method only organizes the swarm in the Two-Dimensional (2-D) space. Therefore, each robot maintains a desired 2-D Euclidean distance from the others while keeping a constant distance from the ground.

4.4 Intra-swarm Relative Sensing

As explained in the previous sections, the information required to achieve and maintain the flocking using our proposed method is the relative range d and bearing ϕ of

each neighbor in the maximum interaction range D_p. Detect and localize nearby neighbors is the key to obtaining the relative range d and bearing ϕ.

To evaluate our method, we use two relative localization approaches. The first approach relies on the exchange of GNSS information inside the swarm through direct communication using Wi-Fi. The second approach consists of a direct vision-based relative localization system called the UVDAR system. Both can obtain the required information to achieve the flocking differing in each circumstance they can be applied and the high-level properties of the swarm. However, the use of the UVDAR System as a relative localization approach is one of the main contributions of this work since we aim to demonstrate that self-organized UAV flocking can be achieved in GNSS-denied environments.

4.4.1 Direct Information Exchange-based approach

In outdoor environments, relative position can be obtained via a combination of GNSS and intra-swarm communication. Global position information obtained via GNSS is communicated between MAVs and then used to extract relative position information (COPPOLA *et al.*, 2020). For each position information received through communication, we calculate the relative range d_i of the ith neighboring robot as:

$$d_i = \sqrt{(x_i - x_f)^2 + (y_i - y_f)^2} \tag{4.12}$$

Where: $[x_f, y_f]^\intercal$ is the 2-D position information of the focal UAV in the world frame, and $[x_i, y_i]^\intercal, i \in \{1, \ldots, m_p\}$ is the 2-D position information of the ith robot inside the maximum interaction range D_p in the world frame.

And we calculate the relative bearing ϕ_i of the ith neighboring robot as:

$$\phi_i = \eta_p - atan2(y_i - y_f, x_i - x_f) \tag{4.13}$$

Where: η_p is the physical heading angle of the UAV in the world frame.

The main advantages of this approach are: low computational and power cost when comparing with others approaches, can work in visually clustered environments, and omnidirectional sensing. However, the dependency on a communication network lowers the upper limit for swarm scalability, due to the bandwidth limitations, and significantly reduces the fault tolerance of the entire system.

Generally, UAV practical approaches use ranging systems based on radio signals transmissions (NGUYEN *et al.*, 2019; BHAVANA; NITHYA; RAJESH, 2017), which in turn is subject to the effects of network congestion and interference. Also, according to Coppola et al. (COPPOLA *et al.*, 2020), external infrastructure is required to provide a communication network. The dependency on external infrastructure limits the swarm

Figure 4 – UVDAR LEDs and cameras

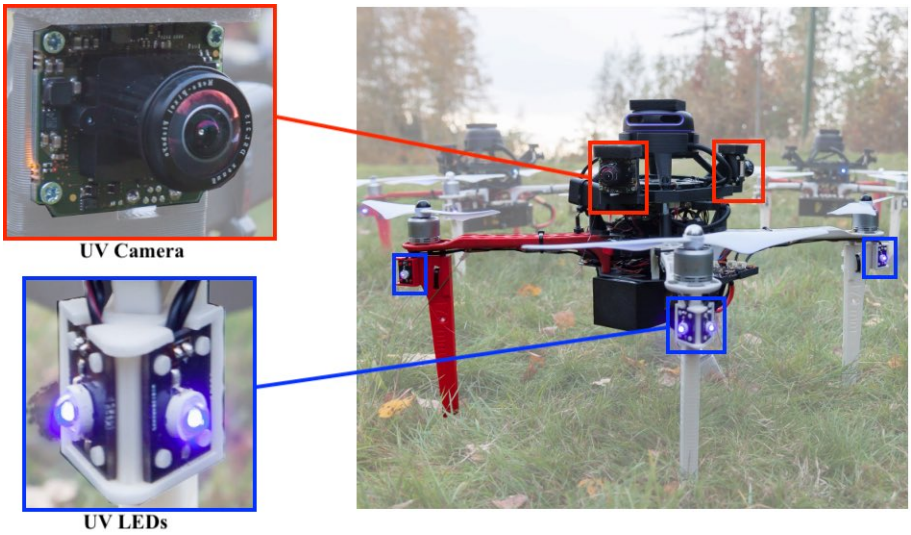

Source: Walter, Saska and Franchi (2018)

to being operable only in areas that have been properly fitted to the task. Several tasks, especially the ones that involve exploration, cannot rely on these methods.

4.4.2 UVDAR system

Traditionally, flocking approaches attempt to replicate, as close as possible, the same behavior found in nature where each individual in the swarm is capable of estimates its neighbor's state by itself, without any communication between them. To accomplish local sensing, we use a direct vision-based relative localization system called the UVDAR system. According to Walter *et al.* (2019), the UVDAR system provides relative position and yaw measurements independently of environmental conditions such as changing illumination and the presence of undesirable light sources and their reflections and does not require communication.

As illustrated in Figure 4, the UVDAR system is based on the application of markers composed of Ultra-Violet (UV) light-emitting diodes on the UAVs, in addition to equipping the observer UAVs with cameras with fish-eye lenses and specialized band-pass filters (WALTER; SASKA; FRANCHI, 2018). To be recognized by the others, a UAV uses pairs of blinking UV-markers attached to its arms. Each pair have a known position around the UAV which makes possible the estimation of the relative position and orientation. A unique frequency in each blinking marker can be used to distinguish each UAV. To recognize the others, a UAV uses two modified cameras with fish-eye lenses providing almost 360° horizontal field of view. The UVDAR system is available as open-source[1].

The use of active markers facilitates the task of detection and increases accuracy.

[1] Repository is available at: <https://github.com/ctu-mrs/uvdar_core>, accessed in June 2021

Also, the independence of communication devices and external computation allows the usage in environments with communication restrictions. As for disadvantages, we have high power expense since it required a few markers and cameras to obtain omnidirectional sensing and may not work in environments where occur occlusion.

Similar to the direct information exchange-based approach (see Equation 4.12 and Equation 4.13), we use the neighbor's position estimated by the UVDAR system to calculate the relative range d and bearing ϕ. However, we do not subtract the focal UAV position from the neighbor's position because the estimation is expressed in the body frame of the focal robot.

4.5 System Architecture

The platforms used in this work consist of several interconnected subsystems, as depicted in Figure 5. The orange blocks represent the relative localization approaches. Only one is active during each experiment. The *Intra-swarm communication* returns the global position information of each near teammates received through Wi-Fi, and the *UVDAR system* block uses the onboard UV-cameras' information to estimate the relative position of nearby teammates. The yellow blocks outline all the mentioned calculations previously. The *Range and bearing extractor* block extracts from each relative position the relative range d and bearing ϕ and then sent to the *Flocking controller*, supplies at 5 Hz. The *Flocking controller* supplies the time-parametrized sequence of the desired position $\mathbf{r}_d$ and heading η_d. The gray blocks depict the essential subsystems to handle basic flight operations. They are part of the Multi-robot Systems (MRS) UAV system, according to Baca *et al.* (2020), is a multirotor UAV control and estimation system created with emphasis on realistic simulations and real-world experiments. A *MPC Tracker* receives and processes the desired position $\mathbf{r}_d$ and heading η_d. This control reference contains the desired position, its derivatives up to the jerk, the heading, and the heading rate, supplied at 100 Hz. Then, a *Position/Attitude controller* receives and provides feedback control of the translational dynamics and the orientation of the UAV. This block creates an attitude rate $\boldsymbol{\omega}_d$ and a thrust command T_d, which are sent to an embedded flight controller[2]. The white blocks stand for the physical design of the UAV. The flight controller encapsulates the underlying physical UAV system with motors and motor electronic speed controllers and creates 4 new controllable DOFs: the desired angular speed around $\hat{\mathbf{b}}_1, \hat{\mathbf{b}}_2, \hat{\mathbf{b}}_3$ and the desired thrust $\langle 0, 1 \rangle$ of all propellers. Finally, onboard sensor data (e.g., position measurements from GPS, velocity measurements from visual odometry) are processed by the *State estimator* and provides the needed information to all these previous blocks.

[2] The proposed system is compatible with the Pixhawk flight controller, installed with PX4 firmware, considering it as already pre-configured with motors, motor speed controllers, and a basic embedded flight controller providing *Attitude rate controller*.

Figure 5 – A diagram of the system architecture: The orange blocks represent the relative localization approaches. Only one is active during each experiment. *Intra-swarm communication* returns the global position information of each near teammate received through Wi-Fi, and *UVDAR system* block uses the onboard UV-cameras' information to estimate the relative position of nearby teammates. The yellow blocks outline all the mentioned calculations previously. *Range and bearing extractor* block extracts from each relative position the relative range d and bearing ϕ and then sent to the *Flocking controller*. *Flocking controller* supplies the time-parametrized sequence of the desired position $\mathbf{r}_d$ and heading η_d. The gray blocks depict the essential subsystems to handle basic flight operations. They are part of the Multi-robot Systems (MRS) UAV system. *MPC Tracker* creates a smooth and feasible reference $\boldsymbol{\chi}$ for the reference feedback controller. The feedback *Position/Reference controller* produces the desired thrust and angular velocities (T_d, $\boldsymbol{\omega}_d$) for the Pixhawk embedded flight controller. The white blocks stand for the physical design of the UAV. The *State estimator* fuses data from the onboard sensors to create an estimate of the UAV translation and rotation ($\mathbf{x}$, $\mathbf{R}$)

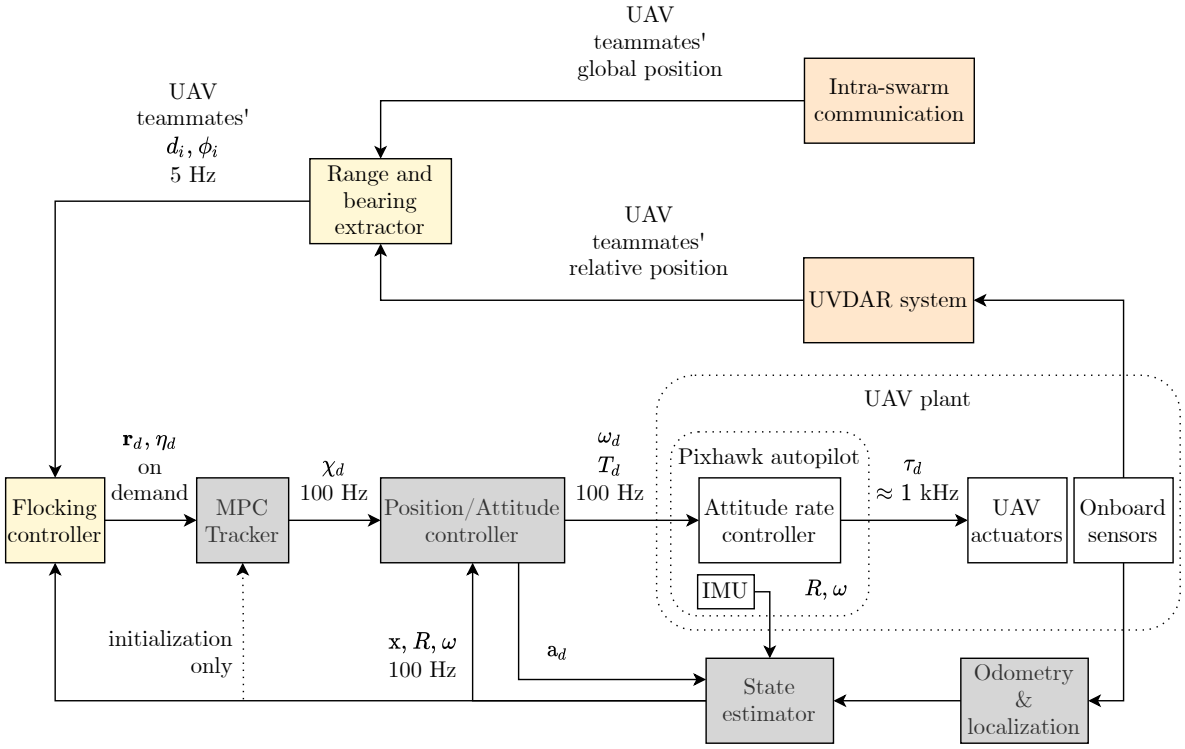

Source: Elaborated by the Author

5 Experimental evaluation

Swarming algorithms usually are applied in a large group of robots (≥ 100). When using ground robots, gathering this high number of robots is somehow feasible. However, in our experiments, we aim to analyze the behavior of autonomous middle-size UAVs, where disturbances from outdoor environments can disturb the group cohesiveness. Thus, we performed real-world experiments with a small number of robots. Before testing our proposed method with real robots, we performed numerous simulations for safe verification and tuning.

In Section 5.1, we explain how our proposed method works and how it was developed by defining the tools used for creating the code. In Section 5.2, we explain the metrics used for determining the performance of our method. In Section 5.3, we describe how the simulations were performed. In Section 5.4, we describe how the experiments with real robots were performed.

5.1 Implementation

Since there is a minimal difference between simulated flight and real-world flight due to the high fidelity simulations of all UAV hardware elements (BACA *et al.*, 2020), the method described in Chapter 4 is implemented almost the same way for simulated and real robots. Each UAV runs an instance of the implementation. The flocking can be accomplished by measuring the relative range d and bearing ϕ of each neighbor inside the maximum interaction range D_p using either the direct communication between the members of the swarm or the UVDAR system. The proposed flocking method is built on Robot Operating System (ROS) and is available as open-source[1].

5.2 Used Metrics

To analyze the effectiveness of our method, we use three metrics. First, we demonstrate how cohesive the swarm aligns in a common direction in a short period using the order metric ψ (VICSEK *et al.*, 1995), which measures the degree of agreement of the orientations of the UAVs within the swarm. Thus, the vectorial sum of the headings of all

[1] Repository is available at: <https://github.com/thulioguilherme/flocking_behavior>, accessed in June 2021

N robots is:

$$\mathbf{b} = \sum_{i=1}^{N} e^{j\phi_i} \tag{5.1}$$

And the order can be calculated as:

$$\psi = \frac{1}{N}||\mathbf{b}|| \tag{5.2}$$

With this metric, the value of the $\psi \approx 1$ defines robots with a common heading. When the value of the $\psi \approx 0$, the robots are point in different directions. We also analyze the steady-state $\bar{\mu}$ (FERRANTE *et al.*, 2012) value for a given metric, which is the order metric ψ in our case. The steady-state metric is the asymptotic value reached by the order metric during the experiment. We can compute the value of the steady-state as:

$$\bar{\mu} = \frac{\sum_{(t=T-100)}^{T} \psi_t}{100} \tag{5.3}$$

Additionally, we use the settling time t^* (FERRANTE *et al.*, 2012), which is the time needed to reach a steady-state in order. More precisely, the settling time t^* is defined as the time for which $\forall t \geq t$ we have $\mu \geq 0.95\bar{\mu}$. In other words, t^* is the time at which and after which the order stays above the 95% of the steady-state.

We can only evaluate our method using those three metrics because we use only the proximal term for calculate the flocking control function. Other metrics used to assess the performance of flocking behaviors, such as accuracy δ and effective traveled distance D_e (FERRANTE *et al.*, 2012), are only measured when the flocking control function incorporates the goal control vector, which is not the case in our method.

5.3 Simulations

In this section, we describe how we performed realistic simulations to evaluate our proposed method. We also explain the experimental setup used and then present the results obtained with both relative localization approaches.

5.3.1 Simulator

We utilized the MRS simulator to evaluate our proposed method through realistic simulations before testing on real robots. According to Baca *et al.* (2020), the MRS simulator is a simulation environment based on the open-source Gazebo simulator with realistic sensors and models that can run in real-time. The MRS simulator is also part of the MRS UAV system. Among the various advantages of the platform, we can highlight:

- Capable of simulate realistic sensors and models in real-time;
- Compatible with multiple versions of the ROS;
- Suitable for swarming researches since scale for multiple UAVs;
- Allow easy transference of simulation settings to real-world experiments.

5.3.2 Experimental Setup

When developing swarm robotics systems, one of the main obstacles is having access to a large number of robots. When performing experiments in simulations and real-world experiments, the available resources restrict the size of the swarm. Due to computational power limitations, we performed simulations with four robots using the direct information exchange-based approach. We used a group of three robots when using the UVDAR system. We kept the same number of robots in the real-world experiments as safety measurements. We consider that the number of robots used is enough to evaluate our method using the following assumptions:

- Putting a number as a lower bound of group size is difficult to justify and swarm robotics should be open to studies with a smaller group sizes, but with a vision of scalability (ŞAHIN, 2005). As presented in the previous chapters, the proposed method aims to be scalable through local sensing and decentralized control;
- The flocking control proposed by Ferrante *et al.* (2012) achieved cohesive self-organized flocking with UGVs using a similar controller configuration, a proximal control and a MDMC control, as the presented in the Chapter 4. They performed numerical analysis with a large number of robots, 1000 simulated and 10 real robots.

To run the simulations, we use a desktop computer with an Intel Core i5-3470 (4-Cores, 6 MB Cache), an Intel HD Graphics 2500 (IVB GT1), and 8 GB (2 x 4 GB) 1600 MHz DDR3 Memory. The simulated robot has a hardware configuration identical to the real one, and all the actuators and sensors are realistic simulated using the MRS simulator. We will discuss the hardware configuration of the robot later in this chapter. For the communication among UAVs, each UAV transmits its global position with a frequency of 2 Hz, which is the expected average frequency in the real-world experiment. The simulated communication does not include loss or delay of transmitted packages.

The proposed flocking method ensures intra-swarm collision avoidance using the proximal term, but it does not have a collision avoidance mechanism between the focal robot and other obstacles. Therefore, as a safety measure, we performed experiments in an open environment to avoid collisions. The simulation environment was composed of a

horizontal plane with no border limits or obstacles. The initial position of each individual was set manually with the restriction that there is at least one neighbor inside the maximum interaction range D_p of each member of the swarm, and the initial inter-distance from each neighbor is higher than the desired inter-robot distance d_{des}. We set the initial heading randomly.

We execute all simulations the same way for both relative localization approaches: after the take-off, the whole swarm hovers and waits for the signal to run the proposed method. Since the expected behavior is to achieve and maintain the flocking, we let each robot run the implementation for a certain period. Most of the parameters are the same for both relative localization approaches, only differing in the desired inter-robot distance d_{des}, which is 6 m for the direct information exchange-based approach and 5 m for the UVDAR system. We summarize the value of the parameters in Table 2.

Table 2 – Parameters values for simulations

Parameter	**Description**	**Value**
B_S	Maximum forward speed	0.3 m/s
κ_1	MDMC linear gain	0.5
κ_2	MDMC angular gain	0.2
α	Steepness of potential function	2
ϵ	Strength of potential function	6
D_p	Maximum interaction range	10.8 m
λ	Interaction range gain	1.8
γ	Interpolation coefficient	0.95
z_{coeff}	Desired height	2.5 m
T	Duration of experiments	240 s

Source: Elaborated by the Author

5.3.3 Results with the Direct Information Exchange-based approach

After the take-off and hovering for a 10 s period, the simulation starts. With only the proximal method proposed here, the UAVs rapidly converged in range and bearing, as can be observed in the settling time t^* of 26 seconds (see Figure 6).

During the simulation, the flocking moved towards an arbitrary direction, as intended (see Figure 7). Once the experiment reaches its duration, the robots are triggered to finish the mission and standstill in their last position. The simulation revealed a steady-state value of $\bar{\mu} = 1.0097$, demonstrating the success of our method, as it indicates that the order assumed values close to 1 during the simulation.

Figure 6 – Order value in the simulation using the direct information exchange-based approach

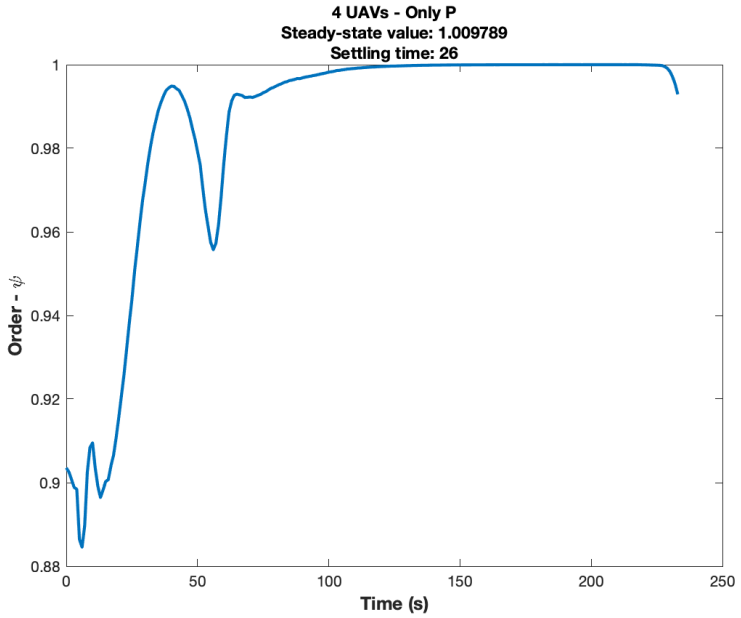

Source: Elaborated by the Author

Figure 7 – XY plot showing UAV headings during the simulation using the direct information exchange-based approach

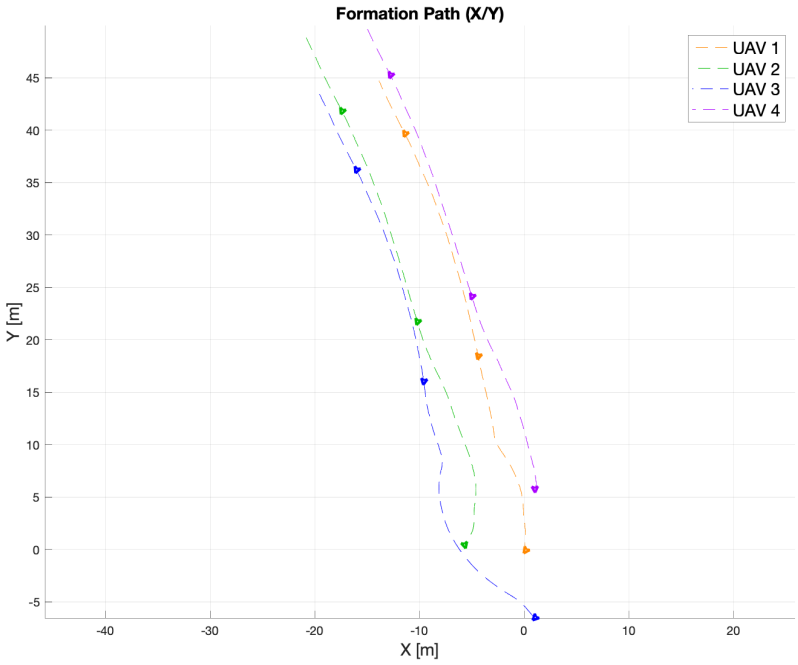

Source: Elaborated by the Author

5.3.4 Results with the UVDAR system

As in the simulation using the direct information exchange-based approach, the swarming starts 10 s after, and again, the UAVs rapidly converge into a cohesive flocking. For a while, the robots converged in range and bearing and moved in an arbitrary direction (see Figure 8), as intended. During the simulation, the swarm was not able to maintain the formation for long periods, which can be noticed in the order's value oscillations and also in the settling time value (see Figure 9). This simulation revealed a steady-state $\bar{\mu} = 0.949469$.

Figure 8 – XY plot showing the heading of the flocking during the simulation using the UVDAR system

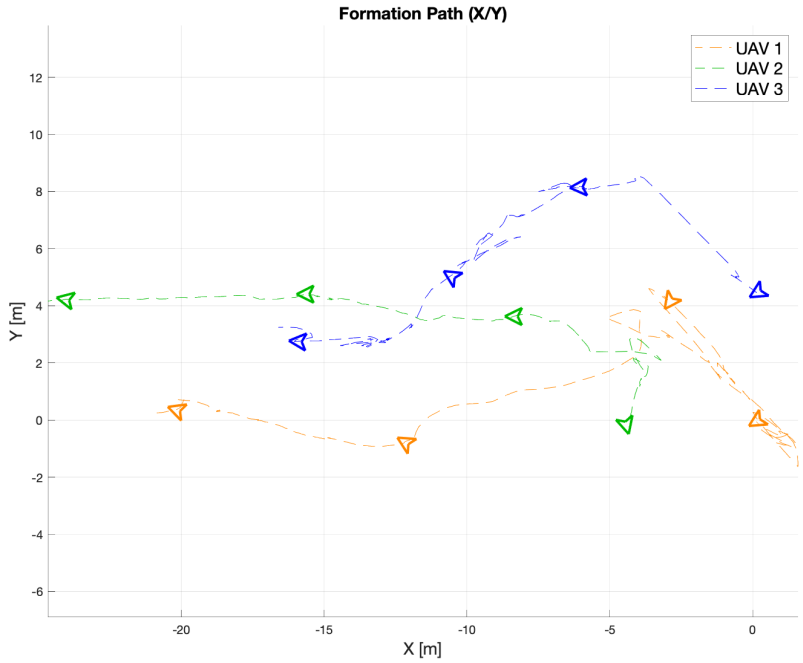

Source: Elaborated by the Author

To better explain the lower result, we first describe a commonly faced issue when attempting to have realistic simulations in the Gazebo simulator. Run realistic simulations is more expensive due to all calculations of physics computation are on a single thread. Due to insufficient processing power, the blinking signals send by the UVDAR LEDs get corrupted, which results in a higher estimation error. It was not possible to have the UVDAR system fully working during the simulation. Despite the issues, the swarm effectively achieved ordered and cohesive flocking, only unsuccessful in maintaining it.

Figure 9 – Order value in the simulation using the UVDAR system

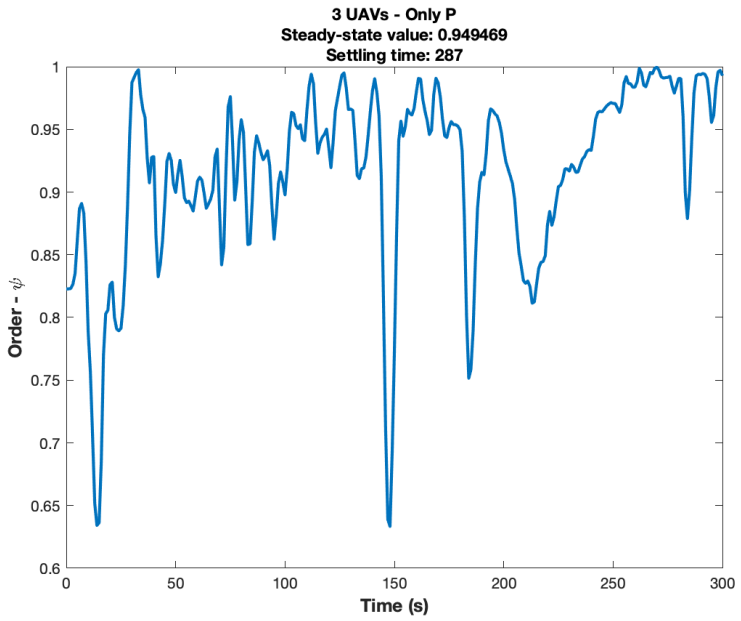

Source: Elaborated by the Author

5.4 Real robots

In this section, we define the components of the UAV used for real-world experiments. Also, we describe the experimental setup, and then present the results obtained with both relative localization approaches.

5.4.1 Hardware

For real-world experiments, we use four identical DJI f450-based quad-copters with T-Motor MN2212 motors. Figure 10 shows the main hardware components of the UAV. As the low-level embedded flight controller, we use a Pixhawk 4 which is composed of a set of sensors: an accelerometer, a gyroscope, a magnetometer, and a barometer. An onboard Intel NUC i7 PC with Linux Ubuntu provides computational power for all required tasks, such as flocking control, state estimation, and motion planning. Communication between the Pixhawk flight controller and the onboard PC is established using MAVlink protocol through a serial line. A down-facing rangefinder Garmin LidarLite V3 retrieves the UAV height above the ground. An Ublox Neo-M8N GPS with a compass estimates the global position and the orientation. A base-station laptop operated by a human supervisor supplies basic commands, such as start or stop the experiment, through the local wireless network to the swarm. When using the UVDAR system, each UAV is also equipped with the actuators and sensors required to recognize and be perceptible by the others as depicted in Section 4.4.2.

Since we decided to perform outdoor experiments, the robots have a GPS as the self-localization system. When using the UVDAR system, the robot does not rely on the GNSS system to achieve the desired swarm behavior. It does not use the GNSS information to obtain the relative range d and bearing ϕ of the teammates. We could replace the remote localization system with small or no changes to the proposed method. In contrast to recent works (KOWNACKI; OŁDZIEJ, 2016; VÁSÁRHELYI *et al.*, 2018), where the communication among robots does not rely on a mesh network, we used a local access point to create a wireless network for achieving intra-swarm communication in real-world experiments. We employed this configuration because it was the available hardware equipment.

5.4.2 Experimental Setup

For the real-world experiment, the environment was an outdoor delimited plain field with no obstacles. The base-station laptop operator suspends the experiment if any robot gets close to the borders. The experiments were performed with the support of the MRS group, which supplied the required equipment and personal knowledge for evaluating our flocking method with real UAVs. We kept the same number of robots for each experiment: four robots for the experiment using the direct information exchange-based approach and three robots with the UVDAR system. The values of the parameters are the same as in the simulation (see Table 2). We used GPS data to analyze the trajectory of the robots.

5.4.3 Results with the Direct Information Exchange-based approach

After the take-off and hovering for a 10 s period, the experiment with four UAVs starts. With only the proximal approach proposed here, the UAVs rapidly converged in range and bearing. We selected this run of experimental evaluation to show a typical problem in which one of the UAVs had a minor inaccuracy in its position estimation that placed the robot within a 1.5 m error in the flocking. However, even with this error in the position estimate, the flocking algorithm was successful in converging the robots into a cohesive group (see Figure 11). A video of the real-world experiment with the direct information exchange-based approach[2] is available on Youtube.

During the experiment, the flocking moved towards an arbitrary direction, as intended (see Figure 12). After reaching the boundary of the workspace, the robots are triggered to finish the mission and land. The experiment revealed a steady-state value of $\bar{\mu} = 0.996$, demonstrating the success of our method, as it indicates that the order assumed values close to 1 during the experiment (see Figure 13).

[2] Video of the real-world experiment with the direct information exchange-based approach available at: <https://youtu.be/S5e0lbQw0aU>, accessed in October 2021

Figure 10 – The main hardware components of the UAV: we use a Pixhawk 4 as a low-level embedded flight controller to control the motors, an onboard Intel NUC i7 PC provides computational power for all required tasks, a down-facing rangefinder Garmin LidarLite V3 retrieves the UAV height above the ground, and an Ublox Neo-M8N GPS with a compass estimates the global position and the orientation of the focal robot

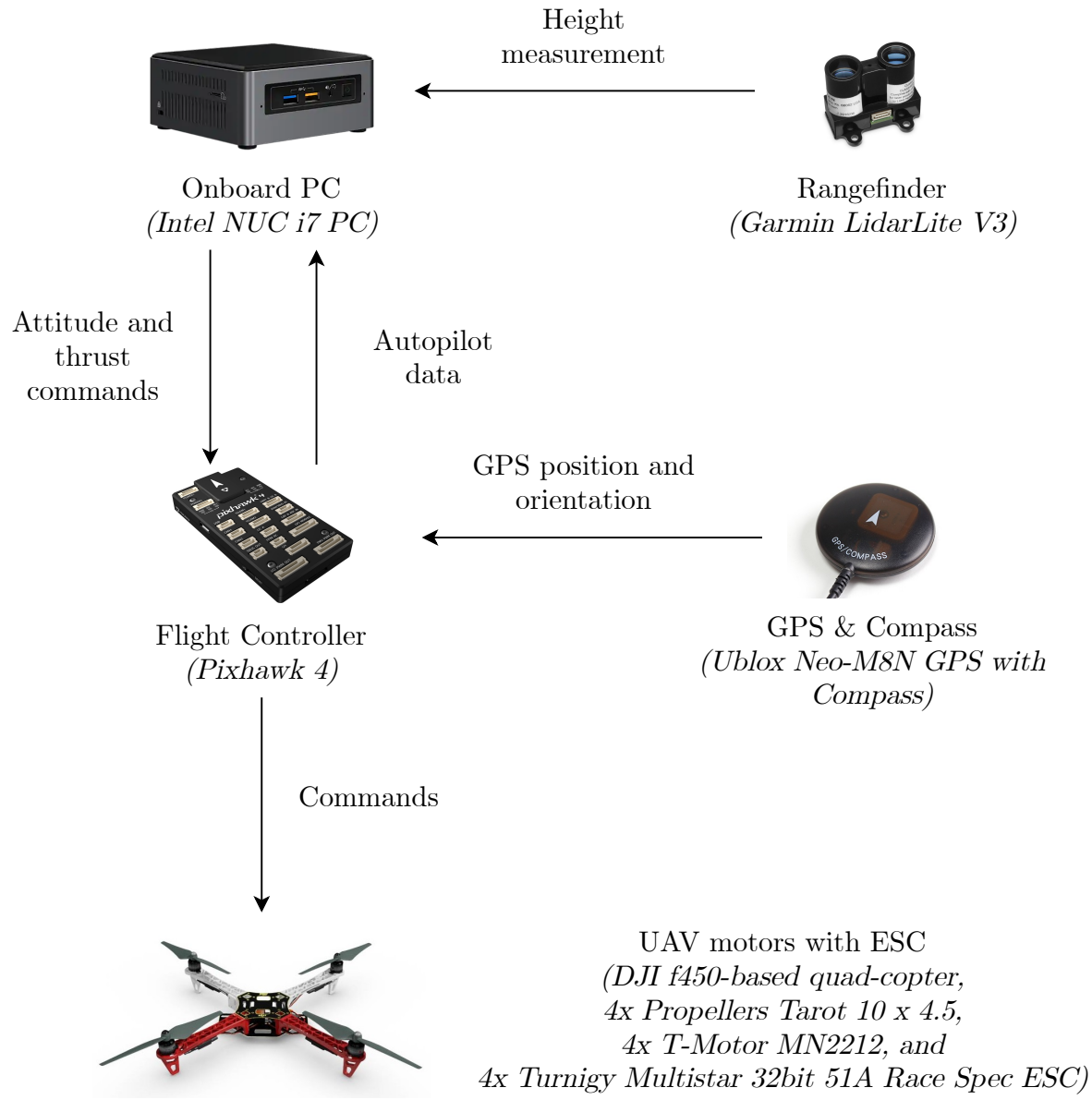

Source: Elaborated by the Author

5.4.4 Results with the UVDAR system

In the experiment with real robots using the UVDAR, the swarming starts 10 s after, and again, the UAVs rapidly converge into a cohesive flocking. Figure 14 present the flocking using UVDAR and the data collected by the UV cameras from two UAVs at the start of the experiment. For a while, the robots converged again in range and bearing and

Figure 11 – The UAVs maintain the flocking up until they reach the field limit

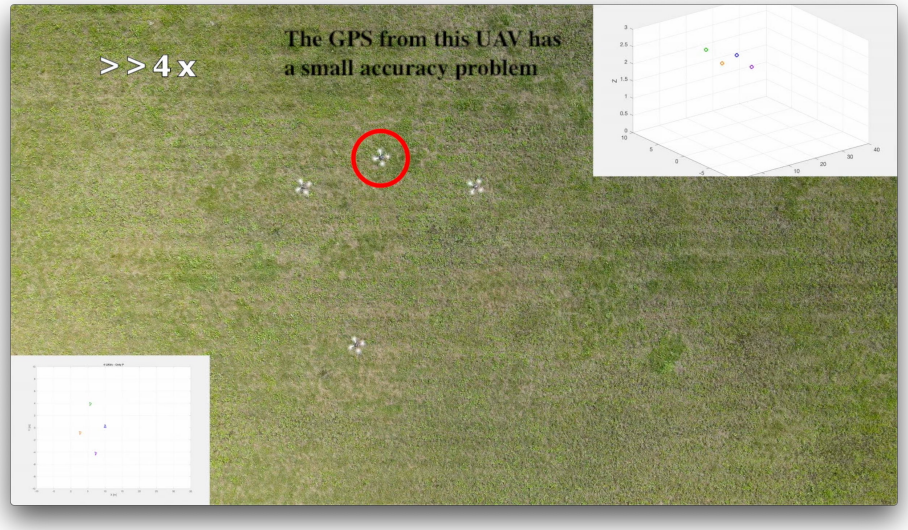

Source: Elaborated by the Author

Figure 12 – XY plot showing UAV headings during the experiment with real robots using the direct information exchange-based approach

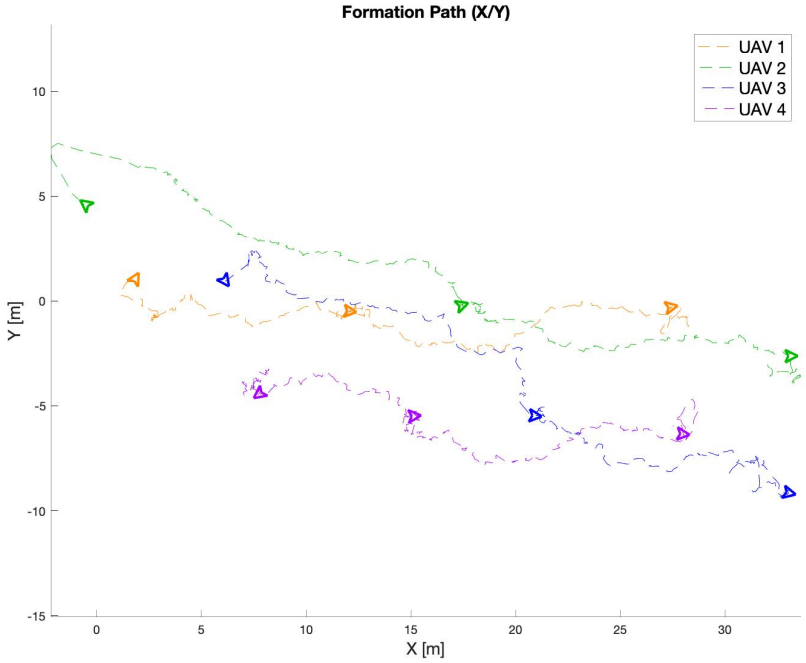

Source: Elaborated by the Author

moved in an arbitrary direction (see Figure 15), as intended. A video of the real-world experiment with the UVDAR system[3] is available on Youtube.

[3] Video of the real-world experiment with the UVDAR system is available at: <https://youtu.be/bJMioc3VgHM>, accessed in October 2021

Figure 13 – Order value in the experiment with real robots using the direct information exchange-based approach

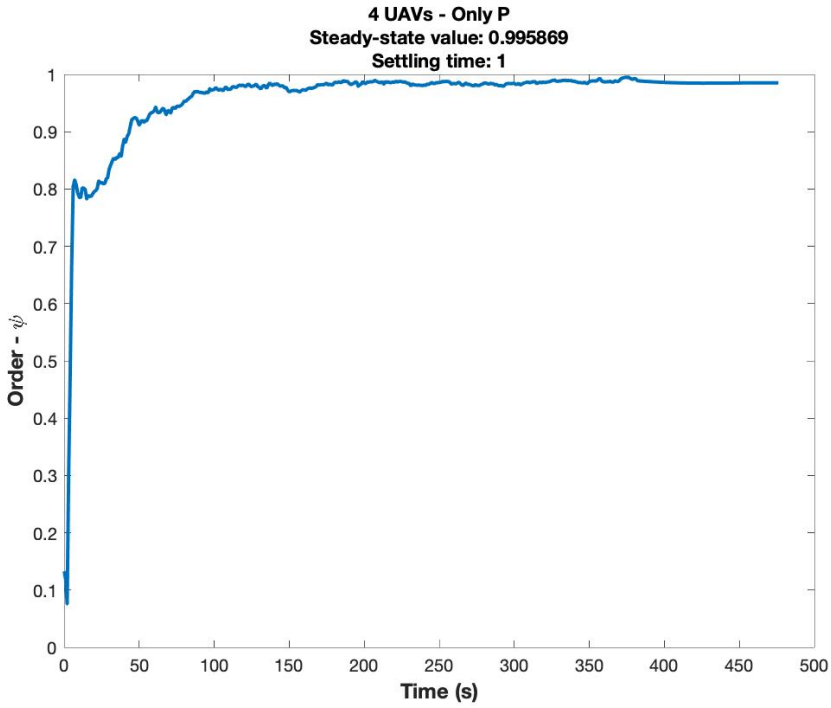

Source: Elaborated by the Author

Figure 14 – During the experiment, each UAV can detect the other robots within the flocking

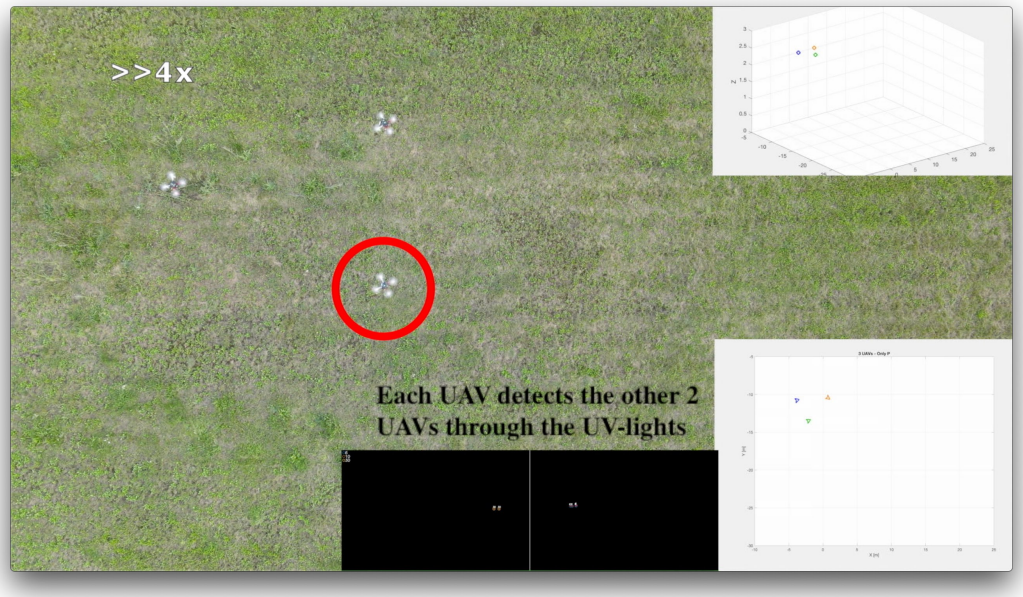

Source: Elaborated by the Author

Figure 15 – XY plot showing the heading of the flocking during the experiment with real robots using the UVDAR system

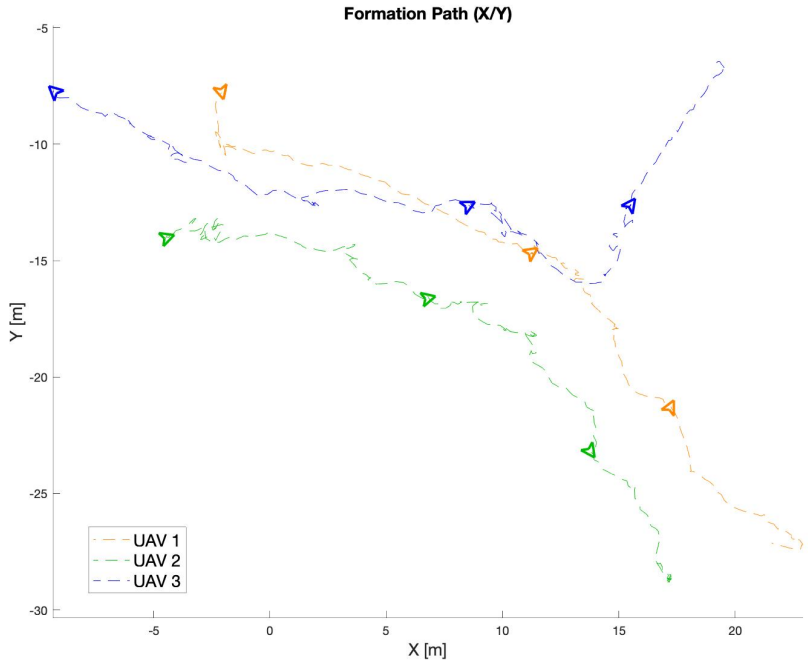

Source: Elaborated by the Author

Figure 16 – Screenshot of the experiment when the blue UAV turns into a blind spot of the UVDAR system

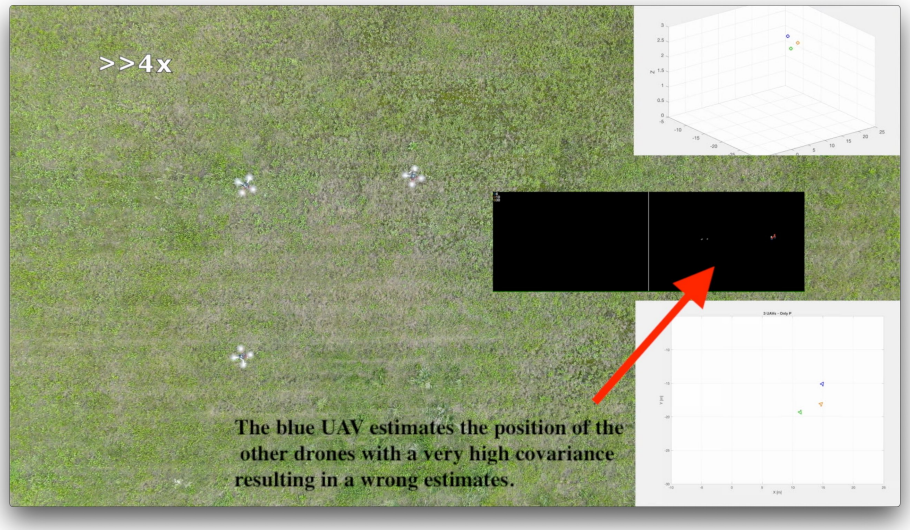

Source: Elaborated by the Author

This experiment revealed a steady-state value of $\bar{\mu} = 0.691870$. To better understand the lower result of the steady-state value, refer to Figure 16, which is a screenshot of the exact moment when the ordered plot diverges (see Figure 17). For a brief moment, the

blue UAV (the UAV at the bottom of Figure 16) changes its heading due to noise in the estimate of the bearing of the other detected UAVs. When performing this move, there is even more noise in the detection. Figure 16 also shows that the detected UAVs move to the edge of the camera. After a while, the UAV can no longer detect the other UAVs because the other robots are in the blind spot region of the UV cameras. Despite the sensory limitations that were purposely shown in this selection of one of the experimental runs, the proposed swarming method was able to stabilize the swarm and achieved the required behavior. This correlates with the results of realistic simulations and with a numerical analysis of the behavior of large swarms (FERRANTE *et al.*, 2012).

Figure 17 – Order value in the experiment with real robots using the UVDAR system

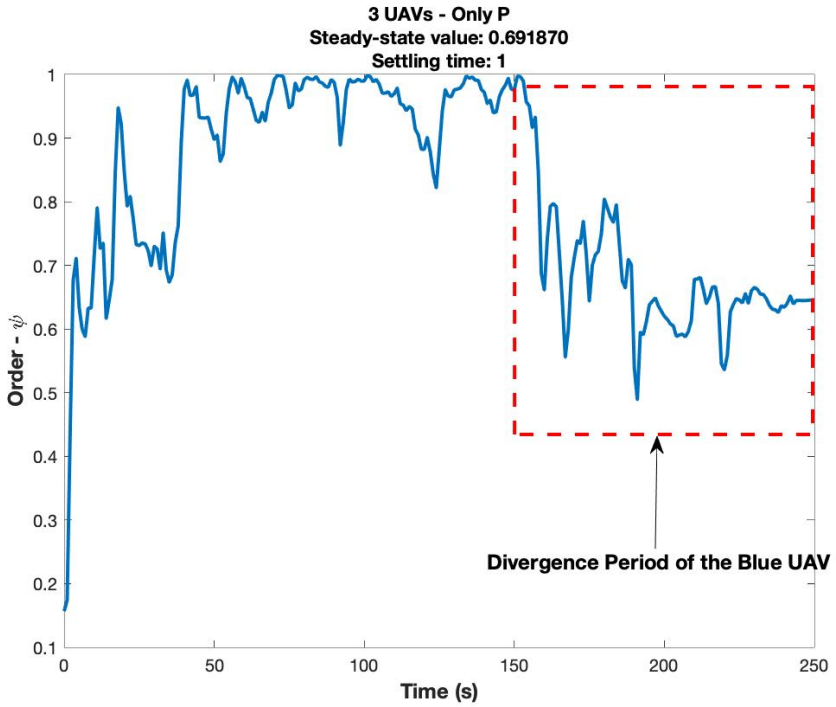

Source: Elaborated by the Author

5.5 Discussion

We focused on developing a decentralized control method to achieve self-organized flocking using middle-size UAVs in GNSS-denied environments. The proposed method accomplishes ordered and cohesive flocking with UAVs following an abstract rule and using minimal information: the robot needs to have non-holonomic movement and senses the relative range and bearing of nearby neighbors.

In the simulated and real-world experiment, our results demonstrated that the proposed method works on UAVs. Despite the estimation errors, the swarm converged into the desired formation and moved in an arbitrary direction, which shows robustness to

inaccurate measurements. Additionally, the proposed method with the UVDAR system enabled the UAVs to achieve and maintain the flocking in a real-world environment using only onboard sensors and processing capabilities.

One of the main contributions is the extension of the work of Ferrante *et al.* (2012) by itself. We adapted their method to work with multirotor UAVs by being robust to larger sensor noise and greater measurement distances. Also, we proposed the use of a spherical linear interpolation function was used as an exponential smoothing technique to deal with the fast angle measurement variations. Similar to Ferrante *et al.* (2012), but apart from the cited UAV works, our work is capable of achieving flocking without the alignment control. Local communication is often used to obtain the advantages of the alignment control but is impractical in some situations. The absence of alignment control leads to a more flexible swarm behavior.

The robot can estimate the required information using remote sensing and intra-swarm communication or using the UVDAR system. The aspect of handle GNSS-denied environments is another contribution. From a swarm robotics perspective, the onboard estimation provided by the UVDAR system is preferable over the intra-swarm communication since it increases the robustness, scalability, and flexibility of the swarm due to the independence of external devices for sensing.

The proposed method achieves flocking in environments with no constraints on the boundary conditions since no collision-avoidance behavior is implemented along with the flocking control. Because the expected behavior of the swarm is to keep an ordered formation while moving forward, tasks that include gathering information from hard-access environments using only onboard sensors are an example of possible applications. As more solid examples, we have parallelized exploration and mapping of environments, and surveys. The proposed method only coordinates the motion of the individuals and could be executed in parallel with another method to retrieve, process, or store the input data.

6 Conclusion

In this work, we have presented a decentralized proximal control-based method to achieve flocking using UAVs in GNSS-denied environments. The proposed method extended the work of Ferrante *et al.* (2012) by adapting a flocking control originally designed for UGVs. We evaluate our proposed method in a real-world environment with a group of middle-size UAVs using two distinct relative localization approaches. The first approach relies on the exchange of GNSS information between the members of the swarm. The second approach uses a direct vision-based relative localization system called the UVDAR system, which can estimate the relative position of the nearby teammates using only the onboard sensors and without communication devices.

The robots converged into a flock formation in the 2-D space, moving in an arbitrary direction with both approaches. The results demonstrated that the UVDAR system can be an alternative to remote sensing. In this way, we achieved self-organized flocking with limited sensory information for aerial robots with high dynamics in environments with no constraints on the boundary conditions. Within the novel flocking method itself, we have provided a framework and guidelines to enable fundamental achievements of swarm research to be integrated into UAV systems working in real-world conditions.

6.1 Publications

To demonstrate the relevance of our work, Table 3 presents the publications that are products of this thesis until the date of October 2021.

Table 3 – Publications that are products of this thesis until the date of October 2021

Work	**Journal/Event**	**Title**
Amorim *et al.* (2021)	2021 International Conference on Unmanned Aircraft Systems (ICUAS)	Self-Organized UAV Flocking Based on Proximal Control
Amorim and Nascimento (2021)	Comunicações em Informática	Self-Organized UAV Flocking Based Only on Relative Range and Bearing

Source: Elaborated by the Author

6.2 Future Works

As future works of this thesis, we have the following possibilities:

- Perform experiments with more robots in simulated and real-world environments to validate the scalability of the proposed method;
- Addition of obstacles as virtual repulsion force inside the flocking control vector. This operation would generate a collision-avoidance behavior along with the navigation behavior, increasing the robustness and flexibility of the swarm;
- Replace the remote self-localization system with an onboard system to achieve complete independence to GNSS.

Bibliography

AMORIM, T.; NASCIMENTO, T. Self-Organized UAV Flocking Based Only on Relative Range and Bearing. *Comunicações em Informática*, v. 5, n. 1, p. 14–17, Jun. 2021. ISSN 2595-0622. Cited on page 53.

AMORIM, T. *et al.* Self-Organized UAV Flocking Based on Proximal Control. In: *2021 International Conference on Unmanned Aircraft Systems (ICUAS)*. [S.l.: s.n.], 2021. p. 1374–1382. Cited on page 53.

BACA, T. *et al.* Model Predictive Trajectory Tracking and Collision Avoidance for Reliable Outdoor Deployment of Unmanned Aerial Vehicles. In: *2018 IEEE/RSJ International Conference on Intelligent Robots and Systems (IROS)*. Madrid: IEEE, 2018. p. 6753–6760. ISBN 9781538680940. Available at: <https://ieeexplore.ieee.org/document/8594266/>. Cited on page 33.

BACA, T. *et al.* The MRS UAV System: Pushing the Frontiers of Reproducible Research, Real-world Deployment, and Education with Autonomous Unmanned Aerial Vehicles. *arXiv:2008.08050 [cs, eess]*, Sep. 2020. ArXiv: 2008.08050. Available at: <http://arxiv.org/abs/2008.08050>. Cited 6 times on pages 29, 32, 33, 37, 39, and 40.

BAYINDIR, L. A review of swarm robotics tasks. *Neurocomputing*, v. 172, p. 292–321, Jan. 2016. ISSN 09252312. Available at: <https://linkinghub.elsevier.com/retrieve/pii/S0925231215010486>. Cited 3 times on pages 19, 22, and 23.

BENEDETTI, M. D. *et al.* A fault-tolerant self-organizing flocking approach for UAV aerial survey. *Journal of Network and Computer Applications*, v. 96, p. 14–30, Oct. 2017. ISSN 10848045. Available at: <https://linkinghub.elsevier.com/retrieve/pii/S1084804517302606>. Cited 2 times on pages 27 and 28.

BHAVANA, T.; NITHYA, M.; RAJESH, M. Leader-follower co-ordination of multiple robots with obstacle avoidance. In: *2017 International Conference On Smart Technologies For Smart Nation (SmartTechCon)*. Bangalore: IEEE, 2017. p. 613–617. ISBN 9781538605691. Available at: <https://ieeexplore.ieee.org/document/8358444/>. Cited on page 35.

BRAMBILLA, M. *et al.* Swarm robotics: a review from the swarm engineering perspective. *Swarm Intelligence*, v. 7, n. 1, p. 1–41, Mar. 2013. ISSN 1935-3812, 1935-3820. Available at: <http://link.springer.com/10.1007/s11721-012-0075-2>. Cited 3 times on pages 19, 22, and 23.

ÇELIKKANAT, H.; ŞAHIN, E. Steering self-organized robot flocks through externally guided individuals. *Neural Computing and Applications*, v. 19, n. 6, p. 849–865, Sep. 2010. ISSN 0941-0643, 1433-3058. Available at: <http://link.springer.com/10.1007/s00521-010-0355-y>. Cited on page 26.

COPPOLA, M. *et al.* A Survey on Swarming With Micro Air Vehicles: Fundamental Challenges and Constraints. *Frontiers in Robotics and AI*, v. 7, p. 18, Feb. 2020. ISSN 2296-9144. Available at: <https://www.frontiersin.org/article/10.3389/frobt.2020.00018/full>. Cited 4 times on pages 19, 23, 28, and 35.

DIEBEL, J. Representing attitude: Euler angles, unit quaternions, and rotation vectors. *Matrix*, v. 58, n. 15-16, p. 1–35, 2006. Cited on page 33.

FERRANTE, E. *et al.* Self-organized flocking with a mobile robot swarm: a novel motion control method. *Adaptive Behavior*, v. 20, n. 6, p. 460–477, Dec. 2012. ISSN 1059-7123, 1741-2633. Available at: <http://journals.sagepub.com/doi/10.1177/1059712312462248>. Cited 16 times on pages 8, 9, 19, 20, 23, 24, 26, 30, 31, 33, 34, 40, 41, 51, 52, and 53.

HETTIARACHCHI, S.; SPEARS, W. M. Distributed adaptive swarm for obstacle avoidance. *International Journal of Intelligent Computing and Cybernetics*, v. 2, n. 4, p. 644–671, Nov. 2009. ISSN 1756-378X. Available at: <https://www.emerald.com/insight/content/doi/10.1108/17563780911005827/full/html>. Cited on page 26.

KHATIB, O. Real-Time Obstacle Avoidance for Manipulators and Mobile Robots. *The International Journal of Robotics Research*, v. 5, n. 1, p. 90–98, Mar. 1986. ISSN 0278-3649, 1741-3176. Available at: <http://journals.sagepub.com/doi/10.1177/027836498600500106>. Cited on page 25.

KOWNACKI, C.; OŁDZIEJ, D. Fixed-Wing UAVs Flock Control through Cohesion and Repulsion Behaviours Combined with a Leadership. *International Journal of Advanced Robotic Systems*, v. 13, n. 1, p. 36, Jan. 2016. ISSN 1729-8814, 1729-8814. Available at: <http://journals.sagepub.com/doi/10.5772/62249>. Cited 3 times on pages 27, 28, and 46.

L'AFFLITTO, A.; ANDERSON, R. B.; MOHAMMADI, K. An Introduction to Nonlinear Robust Control for Unmanned Quadrotor Aircraft: How to Design Control Algorithms for Quadrotors Using Sliding Mode Control and Adaptive Control Techniques [Focus on Education]. *IEEE Control Systems*, v. 38, n. 3, p. 102–121, Jun. 2018. ISSN 1066-033X, 1941-000X. Available at: <https://ieeexplore.ieee.org/document/8361125/>. Cited on page 21.

LEE, H.; KIM, H. J. Trajectory tracking control of multirotors from modelling to experiments: A survey. *International Journal of Control, Automation and Systems*, v. 15, n. 1, p. 281–292, Feb. 2017. ISSN 1598-6446, 2005-4092. Available at: <http://link.springer.com/10.1007/s12555-015-0289-3>. Cited on page 21.

LEE, T.; LEOK, M.; MCCLAMROCH, N. H. Geometric tracking control of a quadrotor UAV on SE(3). In: *49th IEEE Conference on Decision and Control (CDC)*. Atlanta, GA: IEEE, 2010. p. 5420–5425. ISBN 9781424477456 9781424477463. Available at: <http://ieeexplore.ieee.org/document/5717652/>. Cited on page 31.

MAHONY, R.; KUMAR, V.; CORKE, P. Multirotor Aerial Vehicles: Modeling, Estimation, and Control of Quadrotor. *IEEE Robotics & Automation Magazine*, v. 19, n. 3, p. 20–32, Sep. 2012. ISSN 1070-9932. Available at: <http://ieeexplore.ieee.org/document/6289431/>. Cited on page 21.

NGUYEN, T.-M. *et al.* Distance-Based Cooperative Relative Localization for Leader-Following Control of MAVs. *IEEE Robotics and Automation Letters*, v. 4, n. 4, p. 3641–3648, Oct. 2019. ISSN 2377-3766, 2377-3774. Available at: <https://ieeexplore.ieee.org/document/8754725/>. Cited on page 35.

REYNOLDS, C. W. Flocks, herds and schools: A distributed behavioral model. In: *Proceedings of the 14th Annual Conference on Computer Graphics and Interactive Techniques*. New York, NY, USA: Association for Computing Machinery, 1987. (SIGGRAPH '87), p. 25–34. ISBN 0897912276. Cited 3 times on pages 23, 25, and 27.

ŞAHIN, E. Swarm Robotics: From Sources of Inspiration to Domains of Application. In: HUTCHISON, D. *et al.* (Ed.). *Swarm Robotics*. Berlin, Heidelberg: Springer Berlin Heidelberg, 2005. v. 3342, p. 10–20. ISBN 9783540242963 9783540305521. Available at: <http://link.springer.com/10.1007/978-3-540-30552-1_2>. Cited 2 times on pages 22 and 41.

SASKA, M. Large Sensors with Adaptive Shape Realised by Self-stabilised Compact Groups of Micro Aerial Vehicles. In: AMATO, N. M. *et al.* (Ed.). *Robotics Research*. Cham: Springer International Publishing, 2020. v. 10, p. 101–107. ISBN 9783030286187 9783030286194. Available at: <http://link.springer.com/10.1007/978-3-030-28619-4_13>. Cited on page 28.

SHRAIM, H.; AWADA, A.; YOUNESS, R. A survey on quadrotors: Configurations, modeling and identification, control, collision avoidance, fault diagnosis and tolerant control. *IEEE Aerospace and Electronic Systems Magazine*, v. 33, n. 7, p. 14–33, Jul. 2018. ISSN 0885-8985, 1557-959X. Available at: <https://ieeexplore.ieee.org/document/8408892/>. Cited on page 21.

SILIC, M.; MOHSENI, K. Field Deployment of a Plume Monitoring UAV Flock. *IEEE Robotics and Automation Letters*, v. 4, n. 2, p. 769–775, Apr. 2019. ISSN 2377-3766, 2377-3774. Available at: <https://ieeexplore.ieee.org/document/8613865/>. Cited on page 28.

SPEARS, W. M. *et al.* Distributed, Physics-Based Control of Swarms of Vehicles. *Autonomous Robots*, v. 17, n. 2/3, p. 137–162, Sep. 2004. ISSN 0929-5593. Available at: <http://link.springer.com/10.1023/B:AURO.0000033970.96785.f2>. Cited 4 times on pages 23, 24, 25, and 26.

TAN, Y.; ZHENG, Z.-y. Research Advance in Swarm Robotics. *Defence Technology*, v. 9, n. 1, p. 18–39, Mar. 2013. ISSN 22149147. Available at: <https://linkinghub.elsevier.com/retrieve/pii/S221491471300024X>. Cited 2 times on pages 22 and 25.

TURGUT, A. E. *et al.* Self-organized flocking in mobile robot swarms. *Swarm Intelligence*, v. 2, n. 2-4, p. 97–120, Dec. 2008. ISSN 1935-3812, 1935-3820. Available at: <http://link.springer.com/10.1007/s11721-008-0016-2>. Cited 3 times on pages 19, 25, and 26.

VÁSÁRHELYI, G. *et al.* Optimized flocking of autonomous drones in confined environments. *Science Robotics*, v. 3, n. 20, p. eaat3536, Jul. 2018. ISSN 2470-9476. Available at: <https://robotics.sciencemag.org/lookup/doi/10.1126/scirobotics.aat3536>. Cited 3 times on pages 27, 28, and 46.

VICSEK, T. *et al.* Novel Type of Phase Transition in a System of Self-Driven Particles. *Physical Review Letters*, v. 75, n. 6, p. 1226–1229, Aug. 1995. ISSN 0031-9007, 1079-7114. Available at: <https://link.aps.org/doi/10.1103/PhysRevLett.75.1226>. Cited on page 39.

VIRÁGH, C. *et al.* Flocking algorithm for autonomous flying robots. *Bioinspiration & Biomimetics*, v. 9, n. 2, p. 025012, May 2014. ISSN 1748-3182, 1748-3190. Available at: <https://iopscience.iop.org/article/10.1088/1748-3182/9/2/025012>. Cited 2 times on pages 26 and 28.

WALTER, V.; SASKA, M.; FRANCHI, A. Fast Mutual Relative Localization of UAVs using Ultraviolet LED Markers. In: *2018 International Conference on Unmanned Aircraft Systems (ICUAS)*. Dallas, TX: IEEE, 2018. p. 1217–1226. ISBN 9781538613542. Available at: <https://ieeexplore.ieee.org/document/8453331/>. Cited 5 times on pages 8, 9, 19, 20, and 36.

WALTER, V. *et al.* UVDAR System for Visual Relative Localization With Application to Leader–Follower Formations of Multirotor UAVs. *IEEE Robotics and Automation Letters*, v. 4, n. 3, p. 2637–2644, Jul. 2019. ISSN 2377-3766, 2377-3774. Available at: <https://ieeexplore.ieee.org/document/8651535/>. Cited on page 36.